Aalto-yliopisto
Insinööritieteiden
korkeakoulu

Tien Van Nguyen

Surface temperature measurement on wood

Thesis submitted in partial fulfilment of the requirements for the degree of Master of Science in Technology.

Espoo 29.05.2017
Supervisor: Professor Petri Kuosmanen
Instructor: Professor Mark Hughes

Aalto University
School of Engineering

Aalto University, P.O. BOX 11000, 00076 AALTO
www.aalto.fi

Abstract of master's thesis

Author Tien Van Nguyen		
Title of thesis Surface temperature measurement on wood		
Degree programme Master's degree in Mechanical Engineering		
Major/minor Mechatronics/Product Development		**Code** K3001
Thesis supervisor Professor Petri Kuosmanen		
Thesis advisor(s) Professor Mark Hughes		
Date 29.05.2017	**Number of pages** 50+15	**Language** English

Abstract

Wood is a hygroscopic material, which exchanges moisture continuously with the surrounding environment. This process involves heat of sorption phenomenon which is either a releases or adsorption of heat, resulting in temperature change on wood surface, which can potentially be utilized to reduce indoor energy consumption. The main objective of this research was to determine a suitable method and develop a protocol to accurately measure the temperature change on wood surface during exchanging moisture with the ambient environment.

While conventional invasive measurement techniques were not considered to be suitable for this purpose, thermography demonstrated the advantages to measure surface temperature and was thus employed as the main technique to measure the change in wood surface temperature during moisture sorption. The measured protocol was validated experimentally by recording temperature change on pine wood surface which is subjected to a change in relative humidity of the environment instantaneously from relatively 0 to 95%. From experimental results, the anisotropy property in wood clearly showed the influence on the temperature change on pine wood during adsorption. The maximum temperature rise on transverse surface was recorded as approximately 3.6 ± 0.4^{o}C, whereas it was only approximately 1.4 ± 0.4^{o}C in cases of radial and tangential surfaces. The experimental uncertainty obtained from 10 repetitions for each direction surface was considerably lower compared with the estimated uncertainty from literature review as 1.17^{o}C. Therefore, it confirmed the suitable ability of thermography to record temperature change on wood due to the heat of sorption phenomenon.

The measurement protocol established from this study can be applied to investigate the temperature variation occurring from different initial moisture contents during sorption in different wood species. Furthermore, the surface temperature data obtained from the heat of sorption experiments will be significant inputs for numerical models describing the behaviour of a wooden building with higher accuracy.

Keywords Thermography, infrared camera, anisotropy, heat of sorption, adsorption, desorption, emissivity, thermal imaging.

PREFACE

This research was conducted in the Department of Forest Products Technology at Aalto University. It was supported by the Wood Life project [2013-2017] funded by Aalto University within the framework of the Aalto Energy Efficiency Research Programme (AEF).

I would first like to give many thanks to my supervisor, Petri Kuosmanen, and instructors, Mark Hughes, Katja Vahtikari and Anna Dupleix for providing me a high support through all this process. It was a great opportunity and high pleasure for me to work with you and explore the knowledge in wood technology as well as experience from research works.

I also want to thank to my friends Quang Le, Trinh Ha and Hiep Nguyen for providing their supports and checking the thesis manuscripts despite of their busy schedule.

Finally, I would like to express my grateful to my family especially to my wife – Anh Hoang, for motivating me when I ever lost interest and making many sacrifices to give me the time to complete this work.

Espoo, May 2017 Tien Nguyen

TABLE OF CONTENTS

LIST OF SYMBOLS

λ	[μm]	Wavelength
α_λ		Absorptivity at wavelength λ
ρ_λ		Reflectivity at wavelength λ
τ_λ		Transmissivity at wavelength λ
W_λ	[W/m^2]	Radiant emittance at wavelength λ
c	[m/s]	Velocity of light
h	[J.s]	Planck's constant
k	[J/K]	Boltzmann's constant
T	[K]	Absolute temperature
ε		Emissivity
ε_{obj}		Emissivity of an object
σ	[$W/m^2.K^4$]	Stefan-Boltzmann constant
τ_{atm}		Atmosphere transmissivity
T_{ref}	[K]	Reflected apparent temperature

ABBREVIATIONS

ASTM	American Society of Testing and Materials
EMF	Electromotive force
FSP	Fibre-saturation point
HVAC	Heating, ventilation and air conditioning
IRT	Infrared thermography
LDPE	Low-density polyethylene
LWIR	Long-wavelength infrared
MC	Moisture content
MWIR	Mid-wavelength infrared
RAT	Reflected apparent temperature
RH	Relative humidity
RSS	Root-Sum-of-Squares
RTD	Resistance temperature detector

1 INTRODUCTION

1.1 *Background*

Wood is a renewable organic composite with various special properties such as low embodied energy, low carbon impact, and sustainability. Wood has not only been widely employed as a building material but has also been used in numerous applications. Various products originating from wood can be easily found in our daily life. In addition, Green building which is defined as "the practice of increasing the efficiency with which buildings use resources while reducing building impacts on human health and the environment-through better siting, design, material selection, construction, operation, maintenance, and removal-over the complete building life cycle" [1] has a great impact on the amount of wood applications. The rise of this concept further promotes the use of wood in many fields such as construction, indoor design to utilize its sustainable properties.

As a hygroscopic material, wood has the ability to attract and hold water molecules from the surrounding environment. The moisture exchange rate of the process depends on the relative humidity (RH) and temperature of the air and the current amount of water in the wood. In general, wood with low moisture content would adsorb moisture vapour from the air with high RH. Inversely, wood with high moisture content would release moisture vapour to the air in a dry condition [1]. Furthermore, the moisture sorption in wood involves heat of sorption, a phenomenon that is either a release or adsorption of heat [2]. This phenomenon results a temperature change on wood surfaces and shows the potential ability to be utilised to reduce indoor energy consumption [3].

In recent years, there has been increasing interest of saving energy consumption by reducing indoor temperature but at the same time maintaining the inhabitant thermal comfort by controlling the humidity through ventilation system. Extensive researches about moisture-buffering capacity of hygroscopic materials such as wood [4-6] have opened great possibilities that increasing use of indoor wooden-based products not only could improve the thermal comfort and air quality [4] but also could increase the energy efficiency in building [6,7]. Simonson et al.[4] proposed that the permeable interior surfaces of a wooden apartment building have great impact on reducing the indoor humidity variation. For example, the peak humidity can drop by 20% compared with employing impermeable materials. Furthermore, Osanyintola and Simonson [6] suggested that combining a well-controlled heating, ventilation and air conditioning (HVAC) system in a room constructed with hygroscopic material has the potential to save energy directly as well as indirectly by adjusting the ventilation rate and indoor temperature. Woloszyn et al. [8] showed that the use of gypsum-based moisture-buffering materials which is also hygroscopic as wood, combined with a relative humidity sensitive ventilation system, could reduce the mean ventilation load by 30-40% and save 12-17% energy consumption during heating season.

However, in most of these studies, the relation between moisture and heat buffering effect between wood and environment could not be completely taken into account, even though in theory it should be. A lack of data about this complex relation was the main reason. Hamery's simulation model [7] assumed an instantaneous equilibrium between the moisture content of the wood surface and the surround, although the moisture exchange in general is a slow process. Therefore, a better understanding of heat of sorption in wood is needed. Thus, it led to the need to measure the surface temperature due to heat of sorption on solid wood.

1.2 *Research problem*

Heat of sorption in wood is a phenomenon in which wood releases or adsorbs heat during the exchange of moisture with surrounding ambient air. The phenomenon results in a temperature change on wooden surfaces. Even though it is a well-known phenomenon in the wood technology field, there has not been sufficient publications on the wood grain surfaces and species dependence of the temperature fluctuation amplitude. The knowledge of the temperature deviation upon moisture sorption is not only valuable information on wood-moisture relation but also the basis to improve indoor thermal comfort. Furthermore, the data obtained from heat of sorption experiments will be significant inputs for a better numerical model describing the behaviour of a wooden building with greater accuracy.

1.3 *Aim of the research*

The main purpose of the thesis work is to develop a method to accurately measure the surface temperature change on solid wood due to heat of sorption. The goal also includes developing the device to be used in the experiment. In addition, a secondary objective is to validate the feasibility of thermography adoption in measuring wood surface temperature.

1.4 *Scope and limitations of the research*

Within the timeframe of a thesis work, the project had its own boundaries.
Only the protocol to measure temperature change on wood surface due to heat of adsorption was focused on. Additionally, the determination of temperature difference were preferred over the measurement of absolute temperature due to limitation in the accuracy of the available infrared camera (FLIR E60 ± 2^{o}C). Furthermore, anisotropic properties of only one wood species were experimented with the RH variation from approximately 0% to 95%.

1.5 *Research methods*

This work focused on experimental research. A protocol to measure temperature change on wood surface during exchanging moisture with surrounding by thermography was established after carefully reviewing literatures and completing a large number of trial experiments. The viability of the protocol was validated by experimental work on measuring temperature rise on different grain-orientations of pine wood due to heat of adsorption.

1.6 *Thesis's structure*

First, heat of sorption theory and different temperature measurement techniques are reviewed in chapter 2. The techniques commonly employed in research community to measure temperature on wood are also reviewed. The limitation of spot measurement was unsuitable to be employed in this project. Instead, infrared thermography showed more advantages to be adopted. In addition, the fundamental working principles of the novel technique was summarized in sub-section 2.2.3. Important factors and parameters of the measurement process such as emissivity of measured material, reflected apparent temperature were noted. Next, in chapter 3, step-by-step protocols for defining wood emissivity and measuring temperature variation during heat of adsorption were presented. Then, the protocols were validated by experimental work with different grain orientations on pine wood specimens. Finally, the results are presented and discussed on chapter 4 and 5.

2 LITERATURE REVIEW

2.1 *Heat of sorption in wood*

Sorption is a physical or chemical process in which one substance attaches to or detaches from the other one. This process includes both adsorption and desorption processes. Adsorption refers to the adherence or bonding of ions and molecules into another substance's surface while desorption is the reverse process.

In particular, sorption of water in wood describes the processes of uptaking (adsorption) or releasing (desorption) water vapour between the wood surface and the surrounding ambient in order to reach the moisture equilibrium at the border. Those are thermodynamically complex processes, which are endo- or exothermic, resulting in a change on the wood surface temperature [9].

Heat of sorption could easy be misunderstood with latent heat which refers to the amount of energy required for the phase change of a substance without temperature change. Bound water in the cell wall of wood is considered similar to the frozen state of ordinary water, with a lower enthalpy (i.e. at lower energy level) than that of liquid water [10]. However, its enthalpy rises with the increase of wood moisture content (MC) up to fibre-saturation point (FSP). Therefore, the relative energy required to vaporise bound water in wood at low MC is higher than for the same amount of normal frozen water. Time (1998) [10] illustrated these relative energy in Figure 1.

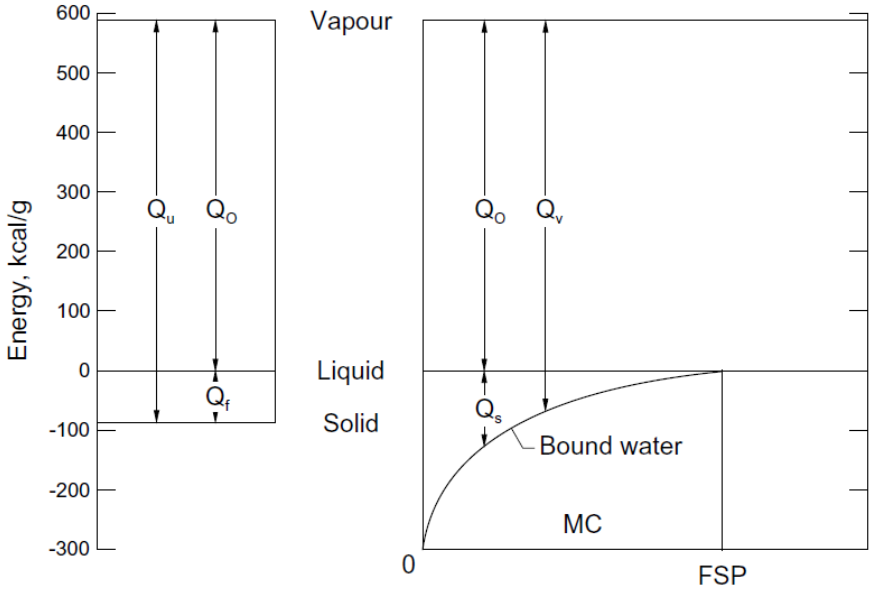

Figure 1 Relative energy levels of water vapour, liquid water, ice and bound water in wood as functions of moisture content, in which Q_o is the relative energy level (r.e.l) of liquid water vaporisation, Q_f is the r.e.l of shifting frozen water to liquid, $Q_u = Q_o + Q_f$ is the r.e.l of frozen water vaporisation, Q_s is the r.e.l of sorption of liquid water by wood (differential heat of sorption), $Q_v = Q_o + Q_s$ is the r.e.l of vaporisation of bound water [10]

In addition, as shown in the Figure 1, the relative energy level (r.e.l) of sorption of liquid water, Q_s, is different than the r.e.l of changing frozen water to liquid, Q_f, and depends on the MC of wood. Also, the difference between Q_s and Q_f is the main distinction between the heat of sorption and latent heat.

In the past, there have been two main methods to determine the differential heat of sorption. The first one is a direct method using different types of calorimeters such as Reaction Calorimeters and Differential Scanning Calorimeters. The other one is an indirect method based on the calculation by Clausius-Clapeyron equation. More discussions regarding this topic can be found in the literature [2,11]. However, the underlying mechanisms behind the heat of sorption phenomenon is still unclear. Regardless of that, the sorption of water in wood leads to a change in temperature which has the potential ability to affect the overall energy balance of a building [3].

2.2 *Temperature measurement in general and particularly in wood*

Temperature measurement is a common research task. The section below presents different proposed temperature measurement methods universally employed in the research community. Thermography has been highlighted as a suitable method to measure surface temperature on wood [3].

2.2.1 Typical techniques to measure temperature

Temperature measurement as a study field has a wide variety of needs and applications. To fulfil this need, different methods and devices have been developed based on various phenomena such as thermoelectricity, temperature dependence with the resistance of electrical conductors, and spectral properties. However, invasive or contact measurement techniques are so far the most common methods due to their wide temperature range, ease of use and high accuracy.

Childs et al. [12] summarized different methods in invasive measurement techniques, which are discussed below.

Liquid-in-glass - Mercury

The classical invasive thermometer is the liquid-in-glass device employing mercury with wide applications in determining the temperature of liquid and gas. The mercury level in the glass capillary rises with increasing temperature and vice versa. By calibrating the change in mercury level with a temperature scale, the temperature of the medium in contact with the thermometer can be determined. In practice, liquid-in-glass thermometers are primarily used in manual applications.

Thermoelectric devices – Thermocouples

A thermocouple is a common temperature measurement device used in laboratories and in various industries due to their simplicity, low cost, robustness, various sizes and wide operating temperature range. However, a thermocouple is less accurate than the resistance temperature device. Even though it is problematic to archive the resolution of less than a degree, their sensitivity, response time and wide working range are adequate for many applications.

The fundamental working principle of the thermocouple is based on the Seebeck effect. When two dissimilar conductors are connected at two junctions differentiated in temperature, an electromotive force (EMF) is produced in the circuit between the conductors. The amplitude of the EMF depends on the conductor's material and temperature differences in the junctions. Thus, the temperature of one junction can be determined from that of the other junction and the circuit voltage.

Electrical resistance devices

Since the motions of both free electrons and atomic lattice vibration in a conducting material depend on temperature, the electrical resistance of a conductor is a function of temperature. This relation is used as working principle for different temperature measurement devices such as resistance temperature detector or thermistor.

Resistance temperature detector (RTD)

Pure metal such as platinum, nickel or copper are commonly used as the conductors in RTDs. Since these materials are fragile, their wires are normally protected by ceramic or glass. The most popular RTD is Pt100, employing

platinum as the conductor. Pt100 has a resistance of 100Ω at 0ºC and 138.4Ω at 100ºC.

The highly accurate relationship between the resistance and temperature of RTD conductor enables precise temperature measurement. In comparison with thermocouples, RTDs are more stable and accurate, but, on the other hand, they are more expensive and less responsive. Thus they are mainly used in applications requiring high accuracy.

Thermistor

Unlike RTDs, ceramics or polymers are employed as conducting materials in thermistors to make them high-resistance devices. Operating thermistors is simpler as no complex wiring configurations is required compared to RTDs. Thermistors offer higher accuracy and sensitivity at the expense of reduced temperature range (typically -90°C to 130°C).

2.2.2 Temperature measurement on wood

Thermocouples are currently the most common devices to measure temperature in solid wood. For example, it is the main device to measure in-depth temperature in solid wood exposed to intense radiant energy in Cone Calorimeter [13,14]. Thermocouples were applicable in these experiments because of the low accuracy levels required, as well as their robustness in high temperature measurement.

However, invasive measurement techniques have many challenges in the measurement of the surface temperature on wood notably due to heat of sorption phenomenon. As an organic natural material, the thermal properties of wood vary from point to point, which means that a large number of measurement probes are required to obtain the average surface temperature on wood. Moreover, wood has a significantly low conductivity coefficient, which could result in slow response-time in invasive methods in which heat transfer from the target to the measured devices is mainly through conduction. Furthermore, a critical requirement in heat of sorption is that the specimen surface should be freely exposed to the environment. Thus, positioning the measuring probe on the wood surface without disturbing the phenomenon is challenging. One option is to place the measured probe through a drilled hole as employed in in-depth temperature measurement [13]. However, heat of sorption in wood is a surface phenomenon [9]. Therefore, placing the probe in the wood would miss the target area.

Due to all of these reasons, invasive temperature measurement techniques were not considered to be suitable in this study. Instead, non-invasive techniques such as thermography showed more advantages for the objective of this project.

2.2.3 Thermography

Thermography in general

The temperature measurement method is based on monitoring infrared radiation emitted by the target with an array of non-contact sensors, converting them into electronic signals and finally transforming them into a thermal image. The systems consists of the target, the environment through which the radiant energy is transmitted, and the infrared camera.

At the beginning, in the form of infrared radiation from the object heat transfer is measured by the array of electronic sensors, which can contain thousands of individual detector elements. For example, the FLIR E60 infrared camera contains 320x240 pixels, which means it has over 76000 detector elements [15]. Each of these elements provides as a spot measurement; the change in their electrical properties can be measured and transformed into digital counts using a built-in readout integrated circuit in the device. This digitized data is then converted into a temperature value and assigned a colour or grey-scale value to display temperature distribution in a detailed false-colour image which is called a thermograms, shown on the device's display or a real-time display in the computer.

With the rapid development of technology in thermography, the infrared image-capture process currently operates rapidly thus several thermal images can be obtained within a short period of time, making it possible to create a high resolution thermal video. This characteristic not only highlights the capability of thermal cameras to easily store a substantial amount of temperature data into a video file, but also shows its extensive potential in measuring surface temperature change on different types of materials with no disruption to the system.

In addition, thermal images produced by this technique are created from individual detector element measurements, therefore, analysing thermal images is notably flexible, especially with the help of the analysis software provided by the manufacturer. For instance, temperature measurement from the detector elements within the thermal image can be read with a spot tool. Consequently, maximum, minimum or average temperature within a specific area of the image can be archived.

The advantages of infrared thermography (IRT) over the other temperature measurement techniques [16] are as follows:

- It is a non-destructive method without disturbance to the measure target.
- Thermal images are constructed by a large number of spot measurements to be easily analysed and stored in a video.
- Both spot and surface measurement could be simply analysed by using the software provided by the manufacturer.
- IRT is harmless, without any bad radiation effect such as X-ray imaging. Therefore, it is suitable for intensive use.

The major drawback of infrared (IR) thermography is its accuracy, which depends on the accuracy of the input parameters e.g. material emissivity and surrounding temperature. This will be discussed more in section 2.2.3.4. Additionally, a good understanding of the interaction between different emitting sources surrounding the target is required to archive a reliable measurement. However, an experienced thermographer can overcome all the obstacles and interpret thermographs correctly [17].

Principles of infrared radiation technology

All objects whose temperature is above absolute zero emits energy in form of electromagnetic radiation. Under a temperature of 1000K, the energy is mainly carried by infrared radiations whose wavelength is bigger than visible light and cannot be observed by human eyes. The emitted radiant intensity depends on the temperature of the material; the higher the temperature, the greater the intensity of the infrared energy emitted. The theory of thermography was reviewed by Usamentiaga (2014) [18] and summarized in the section below.

Absorption, transmission and reflection are the three modes by which radiation is dissipated once it strikes an object. These dissipations in fractions of the total radiant energy are referred as absorptivity, transmissivity and reflectivity of the body. Their relations are shown in Equation 1 with corresponding parameters.

$$\alpha_\lambda + \rho_\lambda + \tau_\lambda = 1 \quad (1)$$

where:
α_λ: spectral absorptance, which is the ratio of the spectral radiant energy absorbed by the object.
ρ_λ: spectral reflectance, which is the ratio of the spectral radiant energy reflected by the object.
τ_λ: spectral transmittance, which is the ratio of the spectral radiant energy transmitted by the object.

In case of an opaque material, whose transmissivity $\tau_\lambda = 0$, the Equation 1 is simplified as Equation 2.

$$\alpha_\lambda + \rho_\lambda = 1 \quad (2)$$

A critical term in radiation sciences, a blackbody defines the material in which the transmissivity and reflectivity are null. All of the energy in form of radiation is absorbed once impinging on it ($\alpha_\lambda = 1$).

Electromagnetic radiation emitted from a blackbody ($W_{\lambda b}$) can be calculated by applying Plack's law, as shown in Equation 3.

$$W_{\lambda b} = \frac{2\pi hc^2}{\lambda^5 (e^{hc/\lambda kT} - 1)} \times 10^{-6} \quad (3)$$

where:

- $W_{\lambda b}$: blackbody spectral radiant emittance at wavelength λ (W/m^2).
- c : velocity of light = 3×10^8 (m/s)
- h : Planck's constant = 6.6×10^{-34} (J.s)
- k : Boltzmann's constant = 1.4×10^{-23} (J/K)
- T : Absolute temperature of a blackbody (K)
- λ : Wavelength (μm)

A family of curves archived from Planck's formula for various temperatures is illustrated in Figure 2. Each curve demonstrates the distribution of spectral radiation emitted by the blackbody at certain temperature. As it can be seen in Figure 2, the distributions have a similar trend. At a particular curve, the radiant emittance is zero at wavelength λ = 0, then increases significantly to a peak value at the maximum wavelength λ_{max} and then decreases sharply toward zero again with larger wavelength. From the graph, higher temperature object emits more radiant energy. In addition, the wavelength of the emitted radiation depends on the temperature of the object; the higher the temperature, the shorter the maximum wavelength occurs. This dependence is important and carefully studied in thermography.

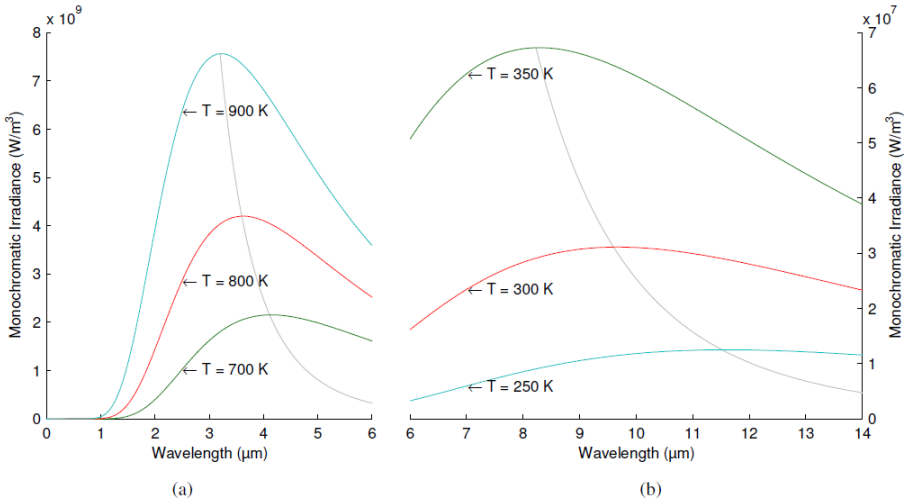

Figure 2 The distribution of electromagnetic radiation emitted from a blackbody at different temperature plotted from Planck's law. (a) Object temperature from 700-900K; (b) Object temperature from 250-350K [18].

Furthermore, the total radiant emittance (W_b) of a blackbody can be obtained by integrating Equation 3 with wavelength $\lambda = 0 \rightarrow \infty$, which is indicated in Equation 4 known as Stefan-Boltzmann's formula.

$$W_b = \sigma . T^4 \qquad (4)$$

The emissivity of a body at a wavelength λ is defined in Equation 5 as the ratio of the radiant energy emitted by the body to that of which would be emitted from a blackbody at the same temperature.

$$\varepsilon_\lambda = \frac{W_\lambda}{W_{\lambda b}} \quad (5)$$

A greybody is defined as an object whose emissivity is constant and independent of the wavelength. Therefore, the emissivity of a greybody can be defined as in Equation 6.

$$\varepsilon = \frac{W}{W_b} \quad (6)$$

The Stefan-Boltzmann formula as Equation 7 for the total radiant emittance of a greybody is obtained by substituting Eq. 4 in Eq. 6.

$$W = \varepsilon . \sigma . T^4 \quad (7)$$

In practice, the emissivity of a real object is not independent of the wavelength; hence, they cannot be considered as a greybody. However, in order to simplify the calculation, an assumption is made that for short wavelength interval, the emissivity can be considered constant. Thus, the real object is considered to be a greybody in a short certain wavelength interval. The Equation 7 is applied for real objects in thermography measurement technique.

In addition, according to Kirchhoff's law which states that a body capable of absorbing all radiation at any wavelength is equally capable in the emission of radiation. Therefore, the emissivity and absorptivity of any material are equal at any specified temperature and wavelength, as expressed in Equation 8.

$$\varepsilon_\lambda = \alpha_\lambda \quad (8)$$

Substituting Eq. 8 to Eq. 2, relation of emissivity and reflectivity of an opaque material can be defined as Equation 9.

$$\varepsilon_\lambda + \rho_\lambda = 1 \quad (9)$$

In case that a greybody is made from an opaque material, Equation 10 can be derived from 9.

$$\varepsilon + \rho = 1 \quad (10)$$

As mentioned previously, since real objects are considered to be greybodies in the short wavelength interval, Equation 10 can also be applied in real opaque objects in a small variation of wavelengths.

Temperature measurement with Infrared Thermography

Bands

Infrared belongs to a part of the electromagnetic spectrum. Its wavelengths are approximately from 0.8µm to 1000µm, situated between visible light and microwave bands. However, not all of the infrared region is used in IRT; in fact, mid-wavelength infrared (MWIR) from 2 to 5 and long-wavelength infrared (LWIR) from 8 to 14 are the most popular infrared regions used in IRT for two main reasons. The first is due to the relation between temperature and wavelength. In order to archive the most efficient measurement, the wavelength region at which the object emits the most intensive radiant energy should be selected. That region should be close to the peak wavelengths shown in Figure 2. Other reason relates to the atmospheric transmittance, in which IR radiations travel from the object surface to the camera detector through the medium also known as the air in most applications. However, certain ranges of infrared wavelength is absorbed through the air, mostly by the particles from CO_2 and H_2O [19].

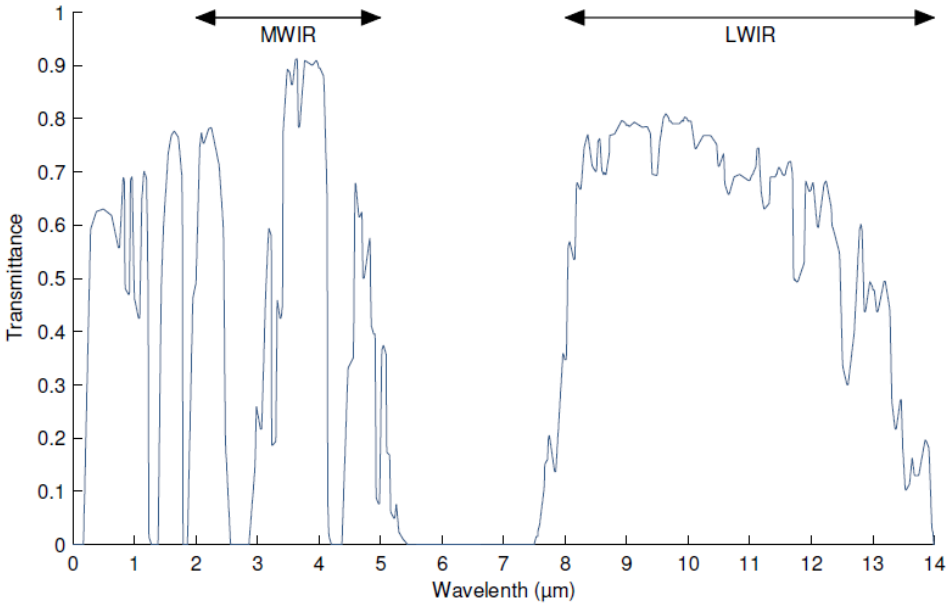

Figure 3 Atmospheric transmittance with different wavelengths at condition T = 15.5°C and RH = 70% [18]

As shown in Figure 3, transmissivity of the wavelength between 5µm and 7µm is extremely low, while in LWIR region, the atmosphere transmissivity is higher at approximately 0.75 in average. Therefore, infrared measuring devices employ either MWIR for high-temperature readings or LWIR for low-temperature readings as ambient temperature.

Radiation detector

Thermal detectors absorb the coming infrared radiation and convert them into electrical signals. The most common detector can be divided into to two main families: uncool microbolometric detectors and cooled detectors.

Formulas in thermography measurement

In temperature measurement with a thermal camera, not all of the radiation absorbed by the thermal detector comes from the target. There exists other sources such as the ambient temperature or surrounding objects contributing to the total radiation as illustrated in Figure 4. In order to archive reliable measurement, these sources should be thoroughly considered in the calculation.

The total energy received by the camera is calculated in Equation 11 which includes the emission from the target (E_{obj}), the emission from the surrounding that is reflected by the target (E_{refl}) and the emission from the atmosphere (E_{atm}).

$$W_{tot} = E_{obj} + E_{refl} + E_{atm} \tag{11}$$

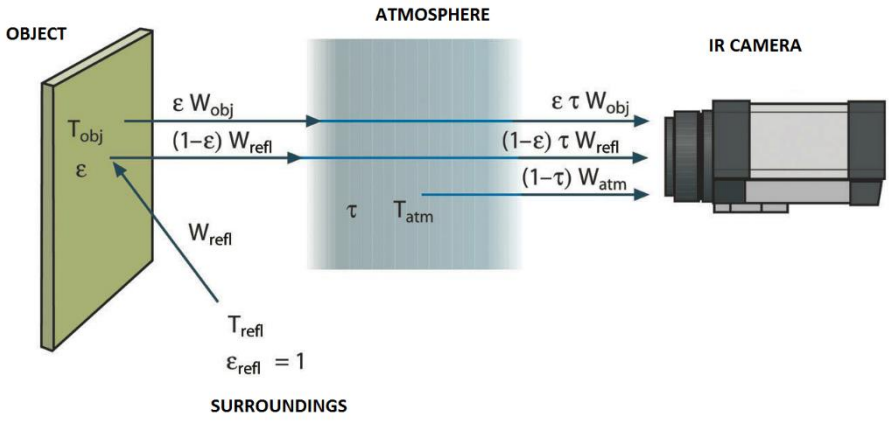

Figure 4 A schematic of the general thermographic measurement [39]

The emission from the target is calculated using the Stefan-Boltzmann formula as shown in Equation 7. In addition, part of the radiation is absorbed by the atmosphere. Thus, it can be expressed as Equation 12.

$$E_{obj} = \varepsilon_{obj}.\tau_{atm}.W_{obj} = \varepsilon_{obj}.\tau_{atm}.\sigma.(T_{obj})^4 \tag{12}$$

Similarly, the emission from the surrounding reflected by the target can be expressed as Equation 13.

$$E_{ref} = (1-\varepsilon_{obj}).\tau_{atm}.W_{refl} = (1-\varepsilon_{obj}).\tau_{atm}.\sigma.(T_{refl})^4 \tag{13}$$

The third part is the emission from the atmosphere which can be expressed in Equation 14.

$$E_{atm} = \varepsilon_{atm}.W_{atm} = (1-\tau_{atm}).\sigma.(T_{atm})^4 \tag{14}$$

Equation 15 is obtained by substituting Equations 12, 13 and 14 to Equation 11:

$$W_{tot} = \varepsilon_{obj}.\tau_{atm}.\sigma.(T_{obj})^4 + (1-\varepsilon_{obj}).\tau_{atm}.\sigma.(T_{refl})^4 + (1-\tau_{atm}).\sigma.(T_{atm})^4 \quad (15)$$

$$T_{obj} = \sqrt[4]{\frac{W_{tot} - (1-\varepsilon_{obj}).\tau_{atm}.\sigma.(T_{refl})^4 - (1-\tau_{atm}).\sigma.(T_{atm})^4}{\varepsilon_{obj}.\tau_{atm}.\sigma}} \quad (16)$$

Therefore, in order to obtain the output temperature from Equation 16, the following parameters must be the input of the device:

- Emissivity of the object.
- Reflected apparent temperature from the surrounding.
- The ambient temperature.
- Relative humidity of the environment.
- Distance from the object to the camera.

In practice, the transmittance of the atmosphere is typically calculated by the analysis software (e.g. FLIR+ software for FLIR products) using the distance from the object to the camera and the relative humidity of the environment.

Furthermore, the emissivity of the object and reflected apparent temperature are the most important parameters for temperature measurement with an IR camera, since the measurement accuracy depends significantly on the uncertainties of these parameters.

Emissivity

Emissivity is the most critical input parameter for IRT. It characterises the capability of a material to emit thermal radiation, compared to that of an ideal blackbody at a certain wavelength. It ranges from 0 to 1 and is calculated by Equation 5.

Emissivity is a surface property and depends on many factors:

- Material
- Temperature
- Wavelength
- Roughness of the surface
- Angle of view from the camera.

Accurate emissivity measurement is essential in low-emissivity materials. As shown in Figure 6 in the next section, in the case of high emissivity objects, slight variation of the emissivity result in only a minor change in the measured temperature. However, in low-emissivity object, any small error in the chosen emissivity would lead to major problem in the resulting temperature [20].

There are different methods to define the emissivity of a material. The easiest way is to look up from table of emissivity provided by certain IR manufacturers or from previous research. However, because of the dependency of many aspects on the application, emissivity must typically be measured. Different standard methods to measure emissivity are defined in the ISO 18434-1 [21]

and the ASTM E1933–99 [22]. At low temperature, the reference emitter method is more popular, in which a reference material with well-defined emissivity such as black electrical tape with ε_{bt} = 0.95 ± 0.05 at 48.8°C [23]. The target is heated to almost the measurement temperature with the reference surface stuck on so that both have the same temperature. Next, emitted radiation from both surfaces is measured by the infrared camera, then the emissivity can be calculated by Equation 17 suggested by Madding et al. [20]. For the purpose of reliable measurement, both target and reference surface should be heated to a temperature at least 20° different to the surrounding.

$$\varepsilon_t = \frac{R_t - R_{ref}}{R_{bt} - R_{ref}} \varepsilon_{bt} \tag{17}$$

In which:

ε_t : emissivity of the target
ε_{bt} : emissivity of the reference emitter
R_t : radiation measured by IR on the target surface
R_{bt} : radiation measured by IR on the reference emitter surface
R_{ref} : radiation measured by IR emitted by surrounding.

Reflective apparent temperature will be described in the next section.

Reflected apparent temperature

The reflected apparent temperature (RAT) is also an important parameter in temperature measurement with IRT, especially for low-emissivity materials. There are two common methods to measure the RAT: the reflector method, and the direct method [21,24]. However, the reflector method is more popular due to the ease of use and the better results produced. In this method, a crumpled and re-flattened piece of aluminium foil is placed on the target surface and in the field-of-view of the IR. The reflectivity of this reference surface is approximately 1, meaning that the surface reflects all the radiation striking it. Therefore, measuring the radiation coming from the aluminium foil with input parameters in IR camera as emissivity of one and distance of zero, the amount of radiation emitted by the surrounding on the target can be defined.

Uncertainty in temperature measurement with thermography

As a measurement, it is important to understand and consider the error in the measurement result compared to the true value, so as to define the result reliability. Also used for this purpose, the degree of uncertainty indicates the estimated upper bound of the measurement error at some level of odds.

Since thermography is a sophisticated measurement system, uncertainty measurement can be significantly challenging. Manufacturers of the infrared cameras usually provide a specification named “accuracy” for each of the products. However, it should be emphasized that this information is given to approximately estimate the uncertainty of all measurement of the object temperature in the working range of the IR camera [25] e.g. -20°C to 120°C for FLIR E60

[15]. It does not precisely define the uncertainty of the measurement with thermal camera for two basic reasons discussed in the following. First, the parameter is normally indicated in the range of ± 2°C or ± 2%; or ± 1°C or ± 1% in the reading of better devices. There are two accuracy ranges, one in Celsius and other in percentage, without any further specification. It is confusing which value should be applied for a certain application as ± 2% error of the reading when measuring an object at 30°C is much less than ± 2°C. Second, the specification is calculated by the uncertainty analysis technique called "Root-Sum-of-Squares" based on partial errors in determining input parameters such as material emissivity, reflected ambient temperature and camera response [20,25]. However, since the uncertainties of these values depend on the user's level of experience and the measuring conditions of the applications, they could not be predicted accurately by manufacturers. Therefore, estimating the uncertainty of the measurement with a thermal camera should be carried out in each applications.

As mentioned before, the uncertainty of the measurement can be calculated from the "Root-Sum-of-Squares" method [20]. The general equation is shown in Equation 18:

$$U_y = \sqrt{\left(\Delta u_1 \frac{\partial f}{\partial u_1}\right)^2 + \left(\Delta u_2 \frac{\partial f}{\partial u_2}\right)^2 + \cdots + \left(\Delta u_n \frac{\partial f}{\partial u_n}\right)^2} \qquad (18)$$

with: $y = f(u_1, u_2, \ldots, u_n)$

Applying Equation 18 to Equation 16, the main error sources of the measurement to be considered are presented below [26]:

- Internal errors of the thermal camera .
- Uncertainty of emissivity measurement.
- Error in reflected apparent temperature determination.
- Error in relative humidity and measured distance determination.
- Error in air temperature measurement.

Internal errors of the thermal camera can be caused by different reasons such as noise in the analog channel, limited resolution of the analog-to-digital converter and transmissivity variation of the optical elements due to the effect of environment temperature [26]. Defining the uncertainty caused by these factors is a complex process and impossible without the help from the product designer. However, most of these systematic errors can be reduced effectively through calibration process; hence, only random error caused by the internal error of the IR camera is considered in the scope of this study.

The material emissivity, the reflective apparent temperature from the surrounding, the air temperature and the RH of the environment as well as measured distance are inputted to the thermal camera by the user. Since they are often detected or measured by different instruments, the uncertainties from these measurements have the main influence to the accurate level of the whole measurement system. Different researches [20,26-28] have focused on studying the contribution from these uncertainty to provide mathematical or experimental

model in order to estimate properly the main uncertainty. The results from these studies have shown that:

- The uncertainty of emissivity contributes dramatically to the total uncertainty compared to others.
- The uncertainty in determining the ambient temperature, the RH of the surrounding and measured distance have small effect to the general uncertainty. In case of short distance measurement, it can be neglected [25,27,28].
- The uncertainty of emissivity contributes much greater to the main uncertainty in case of low emissivity material than in high emissivity material measurement, as illustrated in Figure 6 [20].

In addition, Madding [20] has developed mathematical models to estimate the uncertainty of emissivity measurement with the emitter reference method. Employing a camera with thermal sensitivity of 0.09°F or 0.05°C, the emissivity measurement error can be estimated in Figure 5 depending on the temperature difference between the target and the ambient. For material with high emissivity result i.e. 0.95, the uncertainty of this measurement based on the emitter reference method is approximately 5%

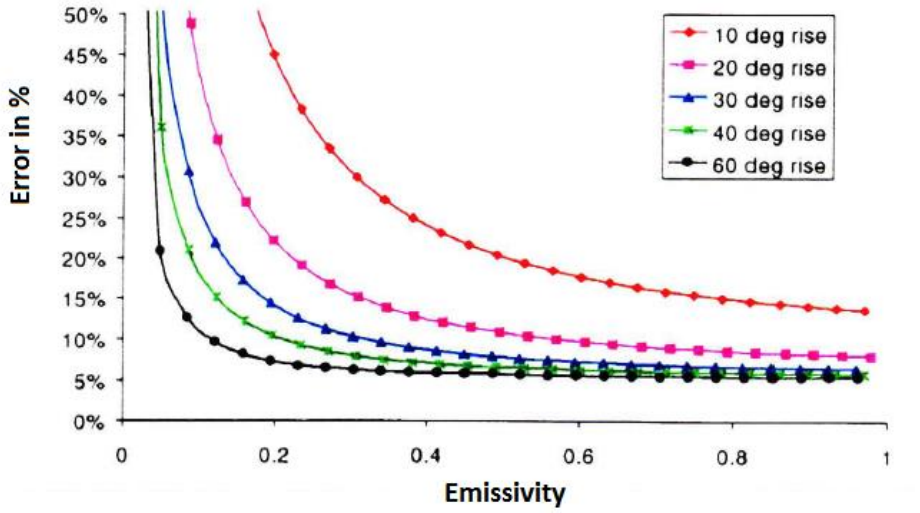

Figure 5 Emissivity measurement error vs. emissivity for various target with temperature rises above background in Fahrenheit [20].

Moreover, Madding has also developed a model to estimate the influence of emissivity uncertainty in the total uncertainty of the temperature measurement with IR camera. For a thermal camera with a thermal sensitivity of 0.06°C and 5% uncertainty in the emissivity value, the total uncertainty of the measurement could be estimated with 99.7% of odds by reading from Figure 6. This model is obtained with the assumptions below:

- Transmissivity of the ambient is considered as 1.
- Uncertainties in RH, measuring distance and the ambient temperature measurement are neglected.
- Linearity in detecting radiations of the IR camera

- Systematic error of the camera is neglected, only random error is considered.

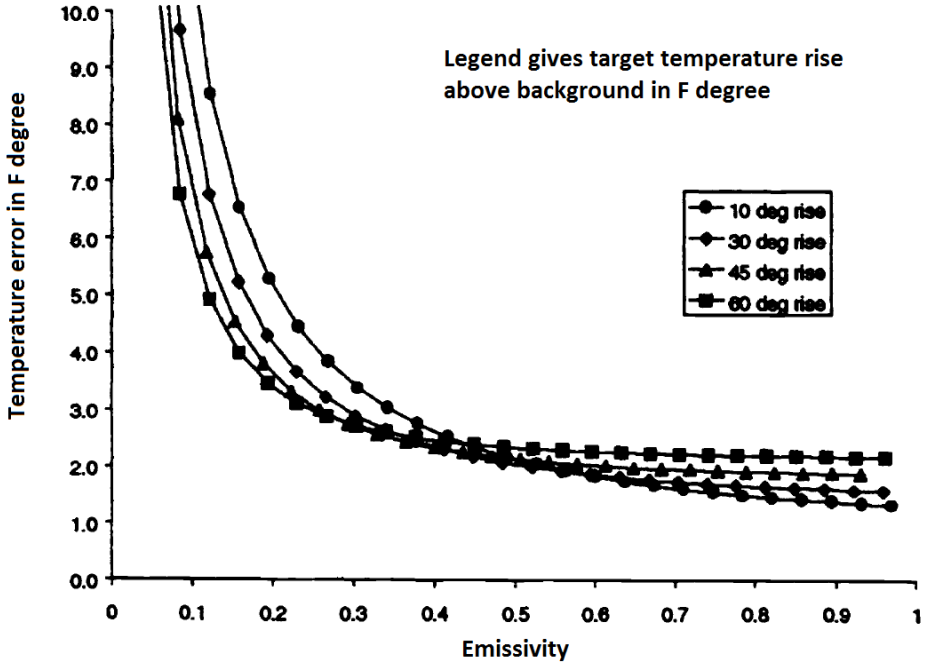

Figure 6 Plots of temperature error vs. emissivity for different temperature rises in Fahrenheit degree above background. Note that the degree unit is in Fahrenheit [20].

This model is a good estimation for the uncertainty of the temperature measurement employing high quality thermal camera.

2.2.4 Application of thermography in research community

The application of thermography has augmented significantly throughout the research community in recent years as the surface temperature measurement has been discussed in various studies. Among other fields, infrared thermography is widely used in building inspection [29] , medicine [30], veterinary medicine [31], maintenance and process monitoring [32] as well as non-destructive testing [33].

IRT is successfully applied in building inspection. Many hidden conditions related to the building performance and maintenance can be observed through thermal imaging. For instance, it can be used to detect air leakage from a building envelope, diagnosis thermal insulation performance [34] or measure the energy efficiency of buildings [35]. Besides, since temperature is a good indicator of health, IRT is also an efficient tool to quickly scan the human body and detect diseases, those have local increase in skin's temperature, such as detecting tumours to early indicate breast cancer [36]. In addition, maintenance is another area where IRT is widely applied. In the electrical field, it is used to indicate faulty connections [37], whereas in the mechanical field, it can indicate excessive friction caused by material fatigue or improper lubrication [38].

2.2.5 Applications of thermography in measuring temperature on wood

Wood emissivity

Wood is an organic composite material with emissivity varying in a wide range depending on species, surface grain orientation and conditions such as temperature, moisture content, wavelengths as mentioned in emissivity study in Section 2.2.3.3. The dependence of wood emissivity on these condition factors will be discussed below.

Emissivity value of wood could be found in some handbook table provided by the manufacturer e.g. Table 1 attained from FLIR user manual [39].

Table 1 Emissivity table from FLIR manual, in which T: total spectrum; SW: 2-5µm; LW: 8-14µm; LLW: 6.5-20µm [39].

Material	Specification	Temperature in ºC	Wavelength	Emissivity
wood	-	17	SW	0.98
wood	-	19	LLW	0.96
wood	planed	20	T	0.80 - 0.90
wood	planed oak	20	T	0.90
wood	planed oak	70	SW	0.77
wood	planed oak	70	LW	0.88
wood	pine	70	SW	0.67 - 0.75
wood	pine	70	LW	0.81 - 0.89
3M type 35	vinyl electrical tape	< 80	LW	0.96
3M type 88	black vinyl electrical tape	< 105	MW	0.96
water	distilled	20	T	0.96
water	layer < 0.1mm thick	0 - 100	T	0.95 - 0.98

As shown in Table 1, wood emissivity at room temperature is in the range of 0.80-0.98 depending on species and wavelength of the emitting radiation. In addition, the emissivity of wood increases along with temperature reduction. However, the experiment's conditions such as ambient temperature, angle of view and moisture content on wood surface are not described properly in the table.

In the existing literature, many researchers have studied the emissivity value of wood. Lopez et al. [22] not only measured the wood emissivity of different species but also analysed this property of pine wood in different conditions with radiant wavelengths from 7.5 to 13µm. Table 2 below shows the emissivity results of pine wood with various natural finishing surfaces used in construction applications subjected to different temperatures.

Table 2 Emissivity for different type of pinewood subjected to different temperatures [23]

Sample test piece	−25 °C	−10 °C	+5 °C	+40 °C	+60 °C
SIL 01	0.985	0.968	0.965	0.938	0.901
SIL 02	0.999	0.991	0.985	0.967	0.927
SIL 03	0.979	0.953	0.951	0.917	0.867
SIL 04	0.963	0.948	0.944	0.900	0.832
SIL 05	0.989	0.976	0.952	0.886	0.850
SIL 06	0.978	0.959	0.947	0.890	0.869

Lopez's experiments confirmed that wood emissivity rises with the decrease in temperature. Emissivity of pine wood with temperature in ranging from 5^{o}-40^{o}C varies from 0.89 to 0.985. However, the dependence of wood emissivity on moisture content was not considered in this study. On the other hand, Kollmann's study [40] suggested that the emissivity of wood increased with its moisture content up to the FSP at which it reached the emissivity of water (0.96) [39]. Dupleix and co-workers [41] confirmed that emissivity of wood with moisture content above the FSP had similar emissivity of water.

In summary, it is discernible that the wood emissivity in certain applications should be measured in order to minimize the uncertainty of wood emissivity and to archive a highly accurate temperature measurement with IR camera. Additionally, studies about this property in wood leads to important notes as below:

- Wood has high emissivity in range from 0.80-0.98.
- The emissivity of wood increases with a reduction in temperature.
- The emissivity of wood increase with a rise in moisture content up to the FSP at which it reaches the emissivity of water.
- At moisture contents above FSP, the emissivity of wood will be similar to the emissivity of water.

Measuring surface temperature on wood with thermography

Thermography has been applied in some researches to measure temperature change due to heat of sorption.

Kraniotis et al. [3] has measured temperature change on untreated wooden surface, in particular Norwegian spruce, while it exchanged moisture with the environment. Both infrared thermography and thermocouple were employed. In their experiments, two spruce heartwood panels were used as the specimens; one had an exposed surface simulating as a permeable surface, while the other specimen had a covered surface with transparent low-density polyethylene (LDPE) foil to prevent moisture exchange simulating as an impermeable surface. Temperatures of the surfaces inside a 41m^3 humidity chamber with RH changing gradually from 0%–90% were monitored at the same time by infrared camera and three thermocouples sets on each surface. Emissivity of spruce wood sample used in this experiments was measured and set at $\varepsilon = 0.90$.

The results confirmed the main role of heat of sorption phenomenon that led to an incremental in the temperature of the wooden surface, as the temperature on the spruce specimen rose much higher than on the impermeable reference specimen. The change is illustrated on Figure 7 below.

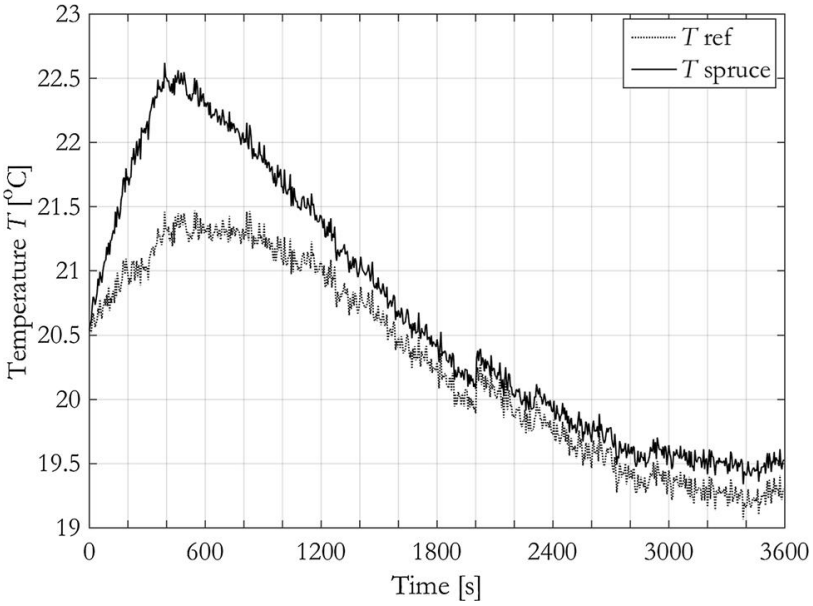

Figure 7 Surface temperature on spruce and reference surfaces in Kraniotis's study [3]

Furthermore, Kraniotis's research has also suggested the suitability of using thermal camera to measure surface temperature of wood comparing to spot measurement. Thermocouples measurement could not be considered, since Kraniotis and co-workers could not be sure if the device was installed correctly to be contact with the wood surface.

However, an issue in Kraniotis's experiment was the instability of interior temperature inside the humidity chamber due to gradual increase in RH from 0-90%. As shown in Figure 8, the temperature inside the chamber increased from 19 to 21°C after 2 minutes and then stabilized at 18.6°C after 15 minutes. The variation in temperature of the environment could affect to the surface temperature change on wood specimen as it affected the temperature on the reference surface. Therefore, the temperature rise detected on wood surface was not only due to the heat of sorption phenomenon. In addition, the uncertainty of the temperature measurement with IRT was not discussed.

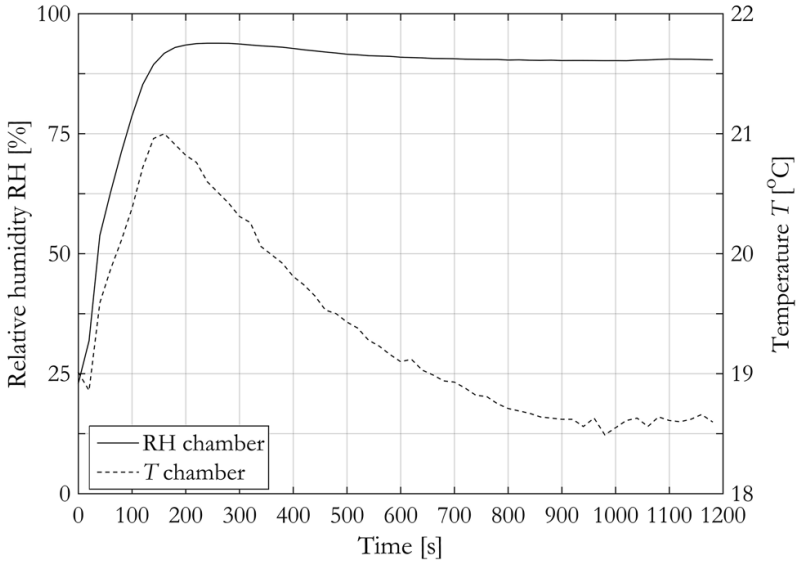

Figure 8 Condition of the climate chamber during heat of adsorption experiment in Kraniotis's study [3]

Similarly, research by Kortelainen [42] investigated surface temperature changes in solid wood during sorption by using also thermography measurement techniques. In this study, different wooden species such as birch, pine sapwood and pine heartwood as well as other grain-orientations surfaces of these species were considered when she measured the temperature changes during both adsorption and desorption. Additionally, the specimens were conditioned so that they were subjected to the variation in RH directly from 0% to 80% or from 32% to 80% in order to study the influence of initial moisture content on wooden surface in heat of sorption. In this study method, both specimen's and climate humidity chamber size were much smaller compared to those in Kraniotis's study. The specimens were prepared in cube shape with 20mm in width. The experiments were conducted inside a climate humidity chamber which is approximately $3m^3$ in volume.

As the result of the study, temperature rise on wooden specimen during adsorption process was observed by thermography. The amplitude of the temperature variation was varied with different grain-orientation of wood surface, notably transverse surface showed the highest rise. Figure 9 shows an example of the results obtained from Kortelainen's research [42].

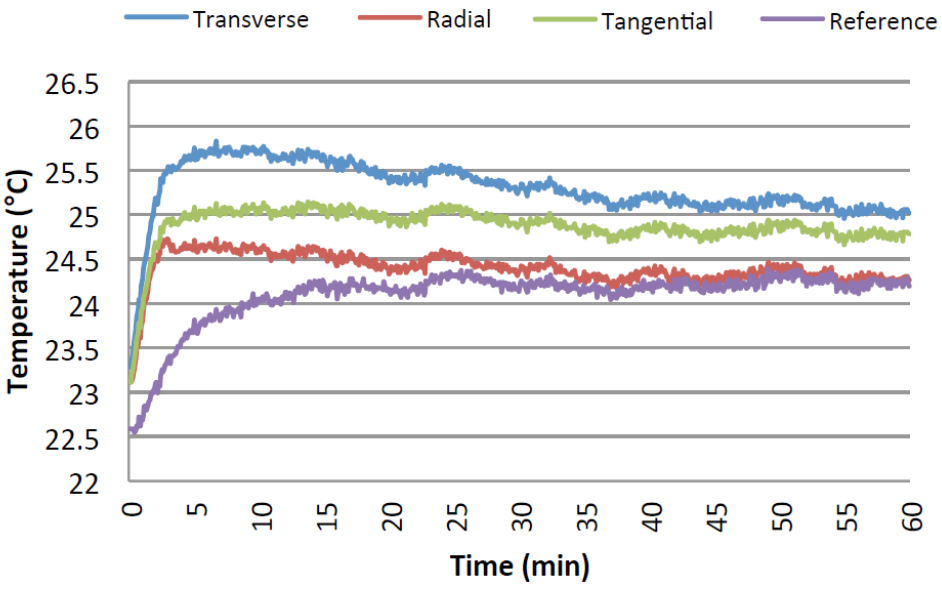

Figure 9 Surface temperature measurement of pine sapwood and reference specimens subjected direct RH variation from 0 to 80% [42]

However, as shown in Figure 9, Kortelainen's experiments also faced an issue with the temperature measurement on the reference surface, which was covered by LDPE plastic film also increased during the adsorption experiment. Several reasons could cause the issue are discussion below

- The specimens were transported outside from one building to another building during winter season in Finland. Even though, the travel distance was short and the specimens were inside a cool box made of Styrofoam, the equilibrium state in temperature on the surface of the specimens could have been interrupted. In addition, the specimens did not have time to stabilize with the new condition in the experimental room.
- The specimens were taken out from the desiccators and weighted before starting the temperature measurement. During this time, the exposed surface of the specimens was in contact with water vapour in the surrounding ambient. Therefore, heat of adsorption had started before the experiment.
- Since the climate humidity chamber employed in this study has a small size, the condition inside the chamber could be significant affected by opening and closing the door.

The issues faced in these previous studies have been carefully considered in the experimental protocol of this study.

2.3 *Summary of literature review*

As a hygroscopic material, wood exchanges moisture with the ambient and leads to the change in surface temperature known as heat of sorption. In order to extend the knowledge on this phenomenon in wood, a proper method to

measure the temperature change on solid wood surface due to the heat of sorption is required.

However, this task faces several challenges. Invasive measurement techniques, the most common temperature measurement methods are not proper methods for this research purpose. On the other hand, thermography has significant advantages to be employed.

- It is surface measurement method, which could tolerate the heterogeneous surface properties of wood with average measurement of the surface.
- It is non-destructive temperature measurement technique thus it would not interrupt to the heat of sorption phenomenon.
- A good thermal camera has high thermal sensitivity, which can detect small changes of temperature.
- Wood is a high emissivity material, therefore, smaller uncertainty of the measurement can be archived with IRT.

However, this measuring technique also has challenges

- Emissivity of wood depends on several factors, which requires careful consideration in the set-up.
- Emissivity measurement is mandatory to archive accurate results in the temperature measurement.
- Uncertainty of the measurement is complex to calculate precisely in some cases.

Additionally, experimental set-up process requires stability of temperature of the environment. Any temperature changes not caused by the heat of sorption phenomenon should be avoided. Moreover, since heat of sorption in wood is a quick-responded process, any delay in the measurement should be optimized.

3 MATERIALS AND METHODS

The experimental work was divided into two sections. First, the emissivity of pine wood with respect to the other grain orientations were defined. The change of wood surface temperature during adsorption was then measured by infrared camera based on the emissivity obtained from the first section.

3.1 *Experimental preparation*

3.1.1 Wood specimen

Pine (*Pinus sylvestris*) wood from southern Finland was used due to its availability at the wood workshop of the Department of Forest Products Technology, Aalto University.

In order to archive the most similar surface properties, all samples were cut from the same board of pine. Surface roughness of the samples were finished only with band-saw cut. A sample sized 50x50x25mm^3 was selected to have an appropriate region of interests on thermograms for analysing purpose.

Since one of the objective was to analyse the anisotropy properties of wood on heat of sorption. The specimens were prepared in three groups of 13, distinguished by the cutting directions of the exposed surface: transverse, tangential and radial. The specimen preparation is illustrated in Figure 10. The grain-orientation will be used to refer to the specimen groups in the following sections.

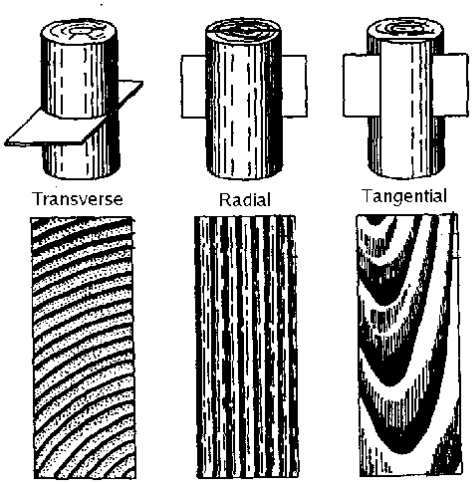

Figure 10 The surface grain orientations of wood [43]

For each group, three samples were prepared for the emissivity measurement experiment whereas the others were employed in the heat of adsorption measurement experiment.

3.1.2 **Humidity chamber**

Heat of adsorption experiment requires a chamber providing high RH at a constant temperature. The device should allow the specimen installation without significantly disturbing the chamber conditions. Additionally, significant changes in the device interior conditions should be monitored during the experiment. A humidity chamber was built and developed for these purposes.

The humidity chamber illustrated in Figure 11 consists of an air-tight 300x300x400mm^3 chamber made from transparent polycarbonate walls, a water tank, two computer fans, two Hygrofox mini data logger, an Arduino Uno, and an ultrasonic mist maker. The data logger close to the sample position inside the chamber acts as the main sensor of the control system, while the other one monitors the exterior condition. All electric devices are connected to a computer controlling the system by a LabVIEW program.

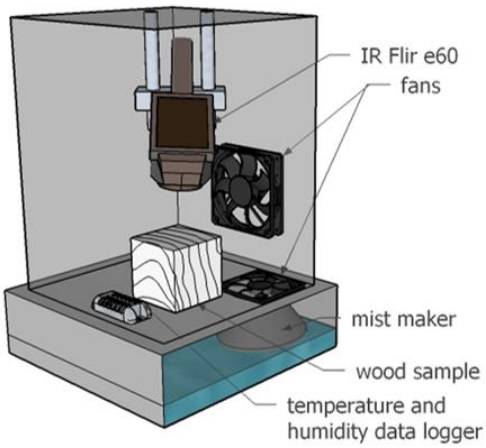

Figure 11 Model of humidity chamber

In humidifier mode, if the reading value of the Hygrofox data logger is smaller than the set point, then the LabVIEW program will turn on the ultrasonic mist maker and the mist-supply fan. Water vapour produced by the mist maker will be directed to the chamber, increasing the moisture level. The devices will be turned off after the set point is reached. Since the vapour produced is at room temperature, the temperature inside the chamber does not vary considerably compared with the outside. The bigger fan constantly circulates the air inside the chamber. The dehumidifier mode applies the same working principle, except that water tank and the mist maker device will be replaced by a silica tank that has low RH condition.

The LabVIEW program contains a user interface (UI) on which humidity target value, speed of the fans can be set as well as real-time values from all the measurement devices can be observed and collected. The accuracy of the RH and temperature sensor inside the data logger is ± 3% in RH and ± 0.4^{o}C in temperature. The mild airflow inside the chamber typically originates from the circulating fan (Antec Tricool model) running at approximately 1600rpm. The chamber door, which is controlled magnetically, is covered with a transparent

plastic film with small cuts in the middle in order to minimize the interference with interior conditions during specimen installation.

3.1.3 Infrared camera equipment

A thermal camera - FLIR E60 was employed in the research due to its accessibility and compact shape to be placed inside the humidity chamber. The camera was positioned inside the humidity chamber by a waterproof handle which does not interfere the moisture sorption process. In addition, the target and the camera were set to a minimum focus distance of about 195mm (confirmed by the experiments) to minimize the effect of air transmission, although it can be compensated by the camera software. Since FLIR manufacturer recommended the maximum angle. Besides, the camera angle of view was fixed to about 25^{o} following the recommendation from FLIR manufacturer respected to the maximum angle of 45^{o}, beyond which significant error would occur in the measurement. The most important specifications of FLIR E60 are indicated in Table 3.

Table 3 Important values of IR camera - FLIR E60

IR resolution	320 x 240 pixels
Spectral range	7.5 to 13µm
Object temperature range	-20 to 120^{o}C or 0 to 650^{o}C
Accuracy	±2°C or ±2% of reading, for ambient temperature 10 to 35°C
Thermal sensitivity	< 0.05°C at 30°C
Detector type	Focal plane array (FPA), uncooled microbolometer

3.2 *Emissivity measurement of dry pine wood*

The main objective of this initial experiment was to measure the emissivity of dry pine wood by the thermal camera E60 for the heat of adsorption experiment. Different grain orientation wood surfaces were analysed. The experiment was performed in accordance to the ASTM E1933–99 [22] employing an electrical black tape as the reference emitter as described in sub-section 2.2.3.

The protocol is demonstrated in Figure 12. At first, wood specimens were dried at 103^{o}C for 24 hours inside the Drying Oven VWR VENTI-Line VL53. A side of their experimental surfaces was then covered with 5 layers of the PVC electrical black tape to minimize the transmissivity of the reference surface to

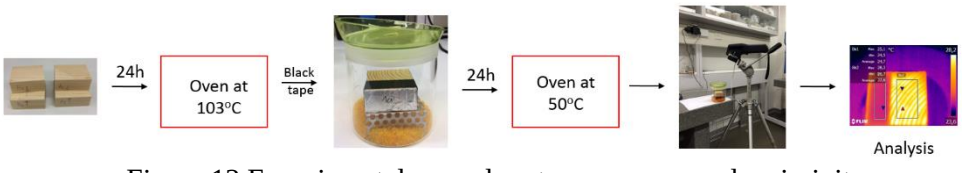

Figure 12 Experimental procedure to measure wood emissivity

relative zero. Subsequently, the samples were transferred into desiccators, with 0% RH, placed inside an oven at 50ºC for another 24 hours.

In the next step, the thermal camera was set on a tripod in such way that it resembled the angle of view and working distance inside the humidity chamber. Afterwards, the desiccator was transferred from the oven to the measuring position. The camera started recording the surface temperature of the black tape and the wood specimen at 30 frame/second immediately after the opening of the lid, which enables the acquisition of the first thermograph after the exposure of wood surface to room condition. The reflected apparent temperature (RAT) caused by the surrounding was then quickly measured with another wood specimen covered by crumble aluminium foil. This final step for RAT was repeated only once per each specimen group, when the emissivity experiments of each group were performed separately.

The average radiation detected on the wood specimen, the black tape and the Al-foil surface were obtained from the thermographs processing by FLIR Tool+ software. The emissivity as 1 and distance as zero were input to the software in this step. Then the emissivity was calculated by Equation 17 as shown in Section 2.2.3.3 with the emissivity of the PVC electrical black tape as 0.95 (± 0.05).

3.3 *Temperature change measurement on wood surface during adsorption*

The experimental goal was to measure the temperature rise on the dry pinewood surface due to heat of adsorption with regard to wood anisotropy property. The main challenge of the setup process was to exclude the temperature change originated from other heat transfer inside the humidity chamber than the heat of adsorption phenomenon. Also minimizing the delay in temperature measurement was important. However, experience acquired from previous studies and a large number of trial experiments have tackled the problems. Some important notes obtained from the initial experiments are listed below:

- The specimens should be placed inside the humidity chamber before the experiment in order to stabilise with the new condition. However, at the same time, their exposed surfaces should be covered to prevent direct contact with the high RH condition.
- The wooden surface should be conditioned to be exposed directly to the target RH to avoid the gradual change in temperature with the increase of RH.

The protocol for measuring heat of adsorption is illustrated in Figure 13.

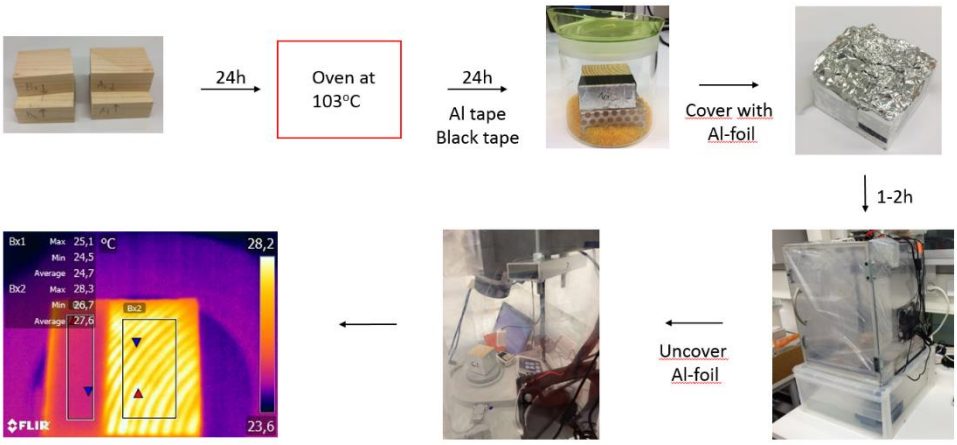

Figure 13 Procedure for heat of adsorption experiments

Initially, wood specimens were dried at 103ºC for 24 hours inside the Drying Oven VWR VL53 to achieve a low wood moisture content. After being removed from the oven, 5 surfaces of the samples excluding the exposed ones, which would be measured by IR camera, were quickly covered with moisture-resistant aluminium tape. Aluminium coverage prevented the moisture uptake from the other sides that would result in the rise of surface temperature, thus interrupting the temperature of the measured surface. Thick layers of PVC electrical black tape were then placed on a side of the exposed surface. In the next step, each sample was preconditioning in a desiccator with ca. 0% RH for 24 hours. During that time, the desiccators were placed next to the humidity chamber in the climate room at 60% RH and 22ºC, so that specimens can reach equilibrium at the same temperature as inside the climate room.

On the main experiment day, the humidity chamber and FLIR E60 were turn on for an hour for the temperature to stabilise. The humidity level was set to 95%. The stabilised condition inside the humidity chamber is shown in the results Section 4.1. The RAT was defined with the same method as in the emissivity experiment. Before placing the specimens into the humidity chamber, their exposed surfaces were wrapped up by an ‘aluminium-foil’ hat in such way that to prevent the surface in contact with the air vapour in the ambient. Additionally, the hat was not only designed to prevent the moisture sorption but also be easy to install and remove on the wood specimens. Small gap between the Al-foil and the specimen was tightened by semi-transparent tape. After one hour stabilising in temperature inside the chamber, the specimen was positioned to the right place with the best view from the IR camera. The hat was quickly removed, and the camera started recording simultaneously. This procedure ensured that the surface temperature changes on the wood specimens were recorded as soon as the surface exposed to the high humidity of the chamber without any interruption from the inner temperature of the chamber. To our knowledge, this level of control had not been employed previously to measure this particular phenomenon.

4 RESULTS

4.1 *Emissivity of dry pine wood*

Figure 14 illustrates a representative thermograph captured during emissivity experiment. The image indicates the good focus point set for the thermal camera by showing all pure edges of a transverse sample.
Anatomical features of the specimen, such as the growth rings, are visible on the right hand side of the image. The emissivity of late wood and early wood are distinguishable. The black PVC tape, employed as reference surface to indicate the condition inside the humidity chamber during the experiment is also shown on the left hand side.

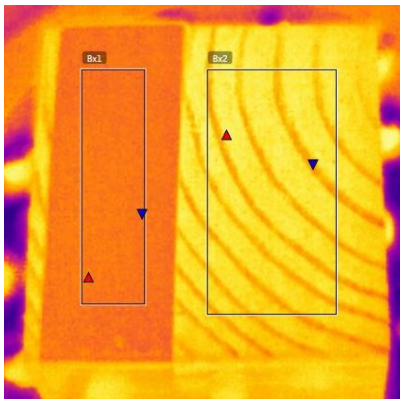

Figure 14 Thermograph of a transverse surface taken during the heat of adsorption experiment (left side covered with Advance® PVC black tape and right side is uncovered).

The emissivity values for each grain orientation on pine wood surface were obtained by following the protocol described in section 3.2. The results are summarized in Table 4.

Table 4 Emissivity results of dry pine wood

Sample group	Emissivity	Standard deviation	COV %
Transverse	0.95	0.01	0.6
Tangential	0.94	0.01	0.6
Radial	0.94	0.01	1

4.2 *Surface temperature rise in heat of adsorption experiments*

In this section, the sample densities and condition inside the humidity chamber are mentioned. Then results of surface temperature change during heat of adsorption on each orientation groups are presented.

4.2.1 **Sample densities and condition inside the humidity chamber**

Table 5 presents the densities of the samples employed in the heat of adsorption experiments. 430kg/m^3 is the representative density with small variation between samples of different orientations.

Table 5 Density values of the heat of adsorption samples

	Transverse	Radial	Tangential	Mean value
Mean (kg/m^3)	428.1	432.2	429.7	430.0
Std deviation	12.4	22.6	16.4	17.4
COV (%)	2.9	5.2	3.8	4.0

The temperature and RH condition inside the humidity chamber recorded by the Hygrofox data logger device are shown in Figure 15. The graph is obtained from one experiment but can be representative of all others when the results were similar.

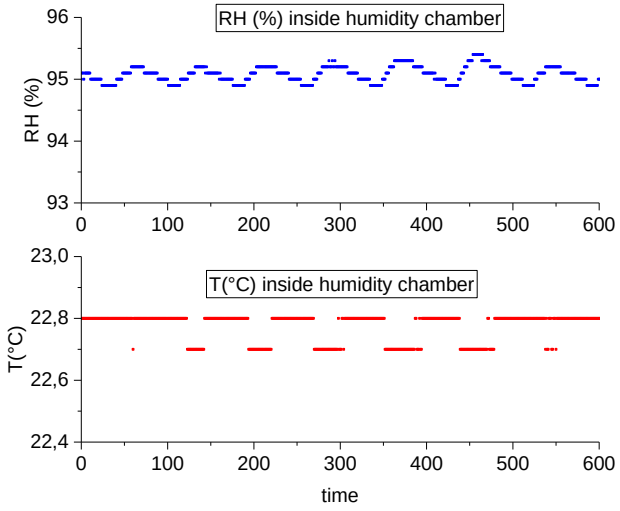

Figure 15 Humidity chamber condition during heat of adsorption experiments.

4.2.2 Temperature rise from adsorption on tangential surface

The temperature changes as a function of time, $\Delta T(t)$, on tangential wooden surfaces during heat of adsorption experiment were recorded and illustrated on Figure 16. It is specified by $\Delta T(t) = T(t) - T_i(0)$ where T(t) is the surface temperature recorded by the camera and $T_i(0)$ is the initial temperature of the sample surface recorded by the camera at t=0. The black curve represents average values of the 10 replicates tested while the red curve is the average plus the standard deviation and the blue curve is the average minus the standard deviation. The mean value of maximum temperature increase on tangential wooden surface is about 1.5°C with 0.3 as standard deviation. The needed time to reach this maximum value is about 48s.

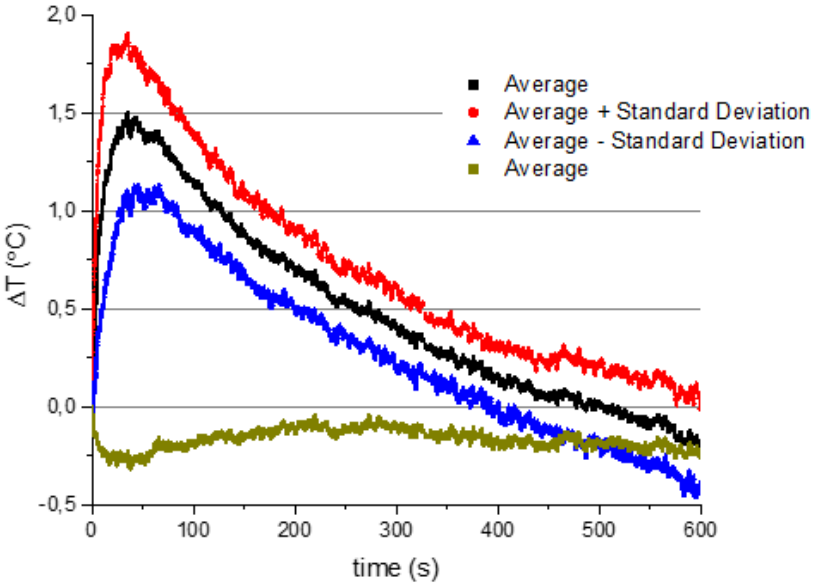

Figure 16 Temperature rise from adsorption on tangential specimens

Surface temperature change on PVC black tape was also recorded at the same time with wooden specimen. Its result is demonstrated by the green curve. It can be seen that black tape surface temperature change are more stable than the wooden one, when it varies only within the range of 0.2°C.

4.2.3 Temperature rise from adsorption on radial surface

Similarly to tangential samples result, the temperature changes as a function of time on radial wooden surfaces during heat of adsorption experiment were recorded and illustrated on Figure 17. The mean value of maximum temperature increase on radial wooden surface is about 1.4°C with 0.3 as standard devia-

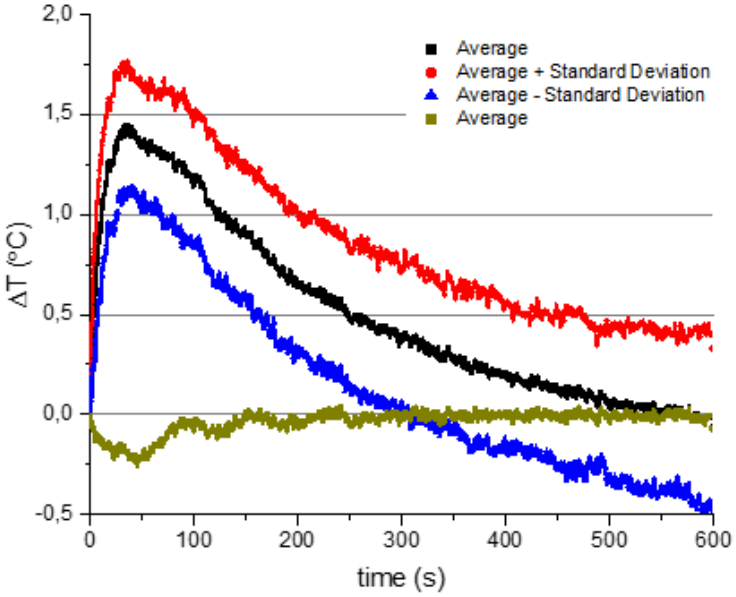

Figure 17 Temperature rise from adsorption on radial specimens

tion. The needed time to reach this average maximum value is about 48s. Although, surface temperature change on black tapes vary within a range 0.25°C during the first 150s, after that it is stable.

4.2.4 Temperature rise from adsorption on transverse surface

Similarly, Figure 18 illustrates the temperature changes as a function of time on transversal wooden surfaces during heat of adsorption experiment. In this graph, also shown is the temperature change on black tape and a wooden surface that was covered by plastic to prevent contact with moisture.

The mean value of maximum temperature increase on transversal wooden surface is about 3.6°C with 0.2 as standard deviation. The time to reach this maximum value is about 282s. Surface temperature change on black tapes gradually increase about 1°C throughout the experiment, while there is no big change on black tape and wooden surfaces that covered by plastic. The temperature variation on the reference surface in this experiment will be discussed more in the next section.

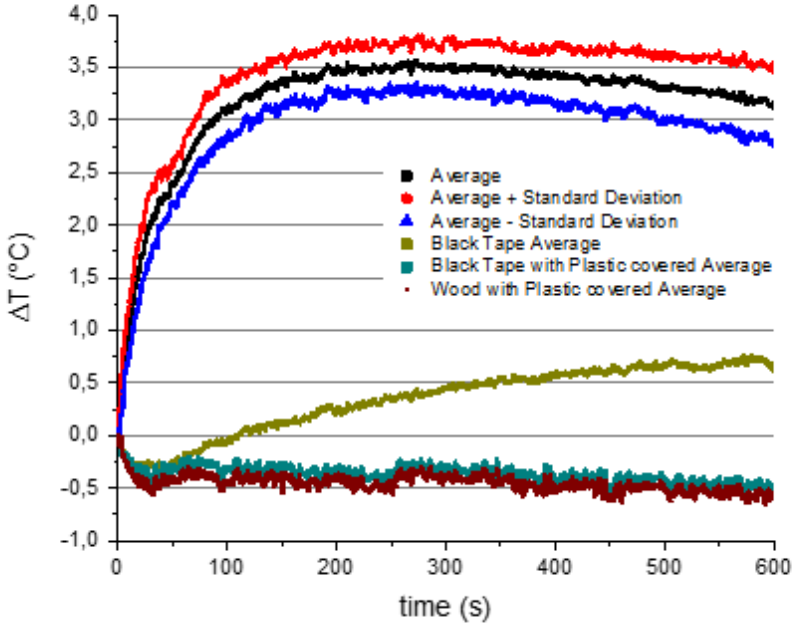

Figure 18 Temperature rise from adsorption on transverse specimens

In summary, the maximum temperature rise and the corresponding time during the heat of adsorption experiment of different grain orientation of pine wood are shown in Table 6.

Table 6 Summary results of heat of adsorption experiments

a. Maximum temperature rise

	ΔT_{max} (°C)		
	Transverse	Radial	Tangential
Mean	3.6	1.4	1.5
Std dev	0.2	0.3	0.3
COV (%)	4.7	19.5	22.0

b. Time to reach the max temperature

	t_{max} (s)		
	Transverse	Radial	Tangential
Mean	282	48	48
Std dev	92	4	6
COV (%)	33	9	13

5 DISCUSSION

5.1 *Emissivity of pine wood*

The results of the experiments show that the emissivity of dry pinewood is in range of 0.94-0.95 regardless of wood grain-orientation. The uncertainty of the value can be estimated by the Madding model [20] shown in Figure 5. For high material emissivity and the temperature rise of approximately 25^{o} degree in the emissivity measurement experiment, there was an uncertainty of 5% in the result or ± 0.05.

Despite that, during the heat of adsorption experiment, emissivity of pine wood could change due to the moisture content variation on the wood surface and temperature difference between the emissivity measurement and heat of adsorption experiments, the same emissivity was employed by the following reasons. First, as discussed in section 2.2.5.1, wood emissivity increased to the same level of emissivity of water at 0.96 [39] with the increase in moisture content up to fibre-saturated point of wood. However, the emissivity result of dry pinewood was close to the emissivity of water. Therefore, it could be assumed that moisture content variation on wood surface during the short time in heat of adsorption experiments had no influence on the emissivity. Second, the temperature difference between the experiments was approximately 25^{o}C. However, as discussed before, emissivity in wood would increase with the reduction of temperature. Hence, wood emissivity at 23^{o}C was higher than the value recorded at 48^{o}C. Therefore, the small variation in emissivity caused by temperature and moisture content variation in heat of adsorption measurement can be neglected or considered as included in the uncertainty estimation of the emissivity.

5.2 *Temperature rise due to heat of adsorption*

From the experimental results, the surface temperature changes, recorded by FLIR E60 thermal camera on different grain orientation surfaces of solid pine wood, were found to be consistent for each of the ten replicates.

In addition, as the stability of the average temperature change curves on black tape surfaces in tangential and radial experimental results (Figure 16 and Figure 17) or on black tape and wooden surfaces while covered with transparent plastic tape on Figure 18, it can validate the stability condition inside the humidity chamber notably in temperature. There were approximately 1^{o}C temperature variation on black tape surface in the experiments for transverse specimens. However, this could be explained as the temperature rise on wooden surface increases sharply, the heat from wood surface might conduct to black tape and cause the temperature rise on the reference surface. Compared to previous results obtained by Kraniotis et al. [3], illustrated in Figure 7, or Kortelainen [42], illustrated in Figure 9, the results acquired in this study was considerably improved, when the temperature change on wood surfaces were undeniably caused by heat of adsorption phenomenon, not by other heat transfer phenomenon happened inside the chamber.

As indicated from the results, the wooden surfaces have a tendency to increase sharply in surface temperature once exposed to the higher RH environment. After a certain time, depending on the orientation of the wooden surface, it would reach to maximum value then decrease slowly to stabilize at the temperature condition of the environment. Temperature rise on transversal samples are more significant compared with tangential and radial samples. It could reach higher mean value of 3.6°C, however, in a longer time. Temperatures on tangential and radial surface rise to a lower maximum of approximately 1.5°C but more rapidly, only in about 48 seconds. This, again, shows the different properties in different orientation of wood, which should be considered carefully while studying wood.

Furthermore, temperature rise on wooden surface due to heat of adsorption can be noticed as a rapid phenomenon at the beginning; therefore, experimental procedure should consider this behaviour wisely. Thermal camera should start recording immediately when the wood exposed with the ambient since even a few second delay could lead to missing a part of the significant rise in the surface temperature change thus results in inaccuracy.

Moreover, the result can be comparable to the earlier research of Kraniotis et al. [3]. In their study, the temperature increase on tangential surface of spruce heartwood in heat of adsorption phenomenon was observed to reach the maximum of 2.1°C after 500 seconds; the peak value is 0.6° higher than the result obtained in this work. In fact, in their procedure, RH condition of the interior was increased from about 20% to 90% during the first 5 minutes of their experiment, which caused temperature fluctuation in the environment; as the results, the temperature rise in the interior environment could have been accumulated and affected to the temperature rise result of the samples surface. That explains why their result had the higher peak and in longer time compared to the result in this study. Additionally, spruce heartwood, as a different material, was used in Kraniotis's work, which would behave slightly differently to pine wood.

5.3 *Uncertainty of the measurement results*

5.3.1 Uncertainty estimation from literature

Since the IR camera employed in this study has similar thermal sensitivity with the one employed in Madding's study [20], estimated uncertainty in the measurement with thermal camera can be defined from Madding model [20] as shown in Figure 6 . For high emissivity material, the uncertainty is approximately about 1.5°F or 0.83°C. Again, it should be noted that in this uncertainty calculation model, the influence of the ambient transmissivity, the ambient temperature and systematic error of the thermal camera are all neglected.

The uncertainty of temperature difference then can be calculated with Root-Sum-of-Squares (RSS) equation, which results in 1.17°C uncertainty.

5.3.2 Uncertainty estimation from experiments

The temperature change due to heat of adsorption measurement was repeated for 10 times. By calculating the standard deviation of the results, estimated uncertainty of the measurement can be derived.

As shown in Table 6, the biggest standard deviation archived when calculating the average temperature change curves was found on radial experimental result. This variation is approximately ± 0.5^{o} while compared to approximately ± 0.4^{o} in the case of the tangential specimens and even smaller in the case of transverse specimens.

Compared to the uncertainty obtained by Madding model [20], uncertainty estimated by the logistic method is smaller. A reason for this could be that during the subtraction to derive the temperature difference, some systematic errors could have been cancelled each other thus reduces the uncertainty of the measurement. In contrast, the uncertainty calculated with RSS method is added to the sum value.

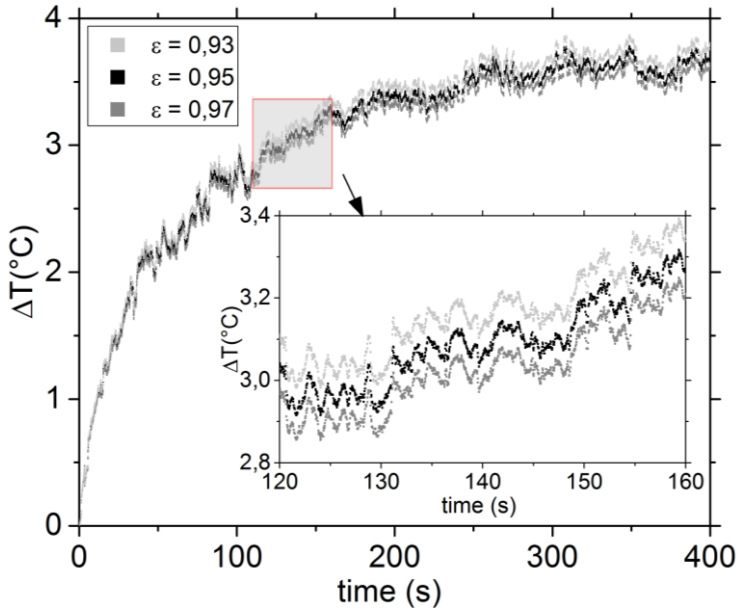

Figure 19 Effect of emissivity on temperature change measurement simulated with FLIR+ software

Moreover, a sensitivity test on the effect of emissivity variation on temperature change measurement, as shown in Figure 19, illustrates that a change in emissivity of ± 0.02 results in only slight changes (less than 0.01^{o}C) in the temperature measurement. It confirms the potential use of thermal camera in temperature measurement for high emissivity material as well as the high accurate results archived from the experiments in this study.

5.3.3 Suggestions for further research

The protocol developed in this study can be considered as a suitable method to measure temperature change on wood during sorption, however, there are sev-

eral ways to improve the accuracy of the measurement. FLIR E60 is a commercial infrared camera, there are other thermal cameras especially developed for research purpose with even higher thermal sensitivity and better accuracy. However, it would require a high budget to purchase these equipment. Additionally, the humidity chamber can be developed further to control also the interior temperature by adding heater and cooler components to the control system. However, it should be designed so that it does not disturb the temperature change on the specimen as well as the heat of sorption phenomenon.

Moreover, the developed protocol can also be applied to measure the temperature changes during desorption on wood. In addition, only one wood species exposed to the extreme RH variation of the environment was considered in this study, it would be interesting to investigate the temperature variation occurring from different initial moisture contents during both adsorption and desorption in different wood species.

Furthermore, the method can also be employed to calculate indirectly heat of sorption in wood. Knowing the temperature changes during heat of sorption on wood surface could provide a boundary condition in a simulation of measuring heat of sorption. However, it would require knowledge on how heat transferred inside solid wood.

6 CONCLUSION

As a result of this study, the validity of using thermography technique to measure temperature change on high emissivity material as wood was confirmed. Contact or invasive measurement techniques are not suitable in these applications. In addition, the protocol to measure temperature change on wood surface due to heat of adsorption was archived and validated by measuring temperature change on pinewood surfaces which were subjected to RH variation from relatively 0 to 95%.

Moreover, anisotropy shows the influence in heat of sorption. Temperature rise during adsorption on transverse surface was considerably higher than that of radial and tangential surfaces. The temperature rise was between 3-4ºC on transverse surface when exposed to high humidity (95%) conditions, whereas it was in range 1-2ºC on radial and tangential surfaces, though the maximum temperature was reached more quickly on these surfaces.

Furthermore, this study confirms the potential ability of using heat of sorption to reduce the energy consumption in buildings. However, more data on temperature rise during sorption for different wood species are required to confirm the feasibility of such application.

REFERENCE

[1] Ross RJ. *Wood handbook: wood as an engineering material*. GTR-190. Madison: WI : U.S. Dept. of Agriculture, Forest Service, Forest Products Laboratory, 2010;508.

[2] Skaar C. Wood-water relations. *Springer Verlag: Berlin, etc* 1988; **283**: 352-353.

[3] Kraniotis D, Nore K, Bruckner C, Nyrud AQ. Thermography measurements and latent heat documentation of Norwegian spruce (Picea abies) exposed to dynamic indoor climate. *Journal of Wood Science* 2016; **62**: 203-209.

[4] Simonson CJ, Salonvaara M, Ojanen T. Improving Indoor Climate and Comfort with Wooden Structures. *Technical Research Centre of Finland, Espoo* 2001; **431**.

[5] Simonson C, Salonvaara M, Ojanen T. The effect of structures on indoor humidity - possibility to improve comfort and perceived air quality. *Indoor air* 2002; **12**: 243-251.

[6] Osanyintola OF, Simonson CJ. Moisture buffering capacity of hygroscopic building materials: Experimental facilities and energy impact. *Energy and Buildings* 2006; **38**: 1270-1282.

[7] Hameury S. Moisture buffering capacity of heavy timber structures directly exposed to an indoor climate: a numerical study. *Building and Environment* 2005; **40**: 1400-1412.

[8] Woloszyn M, Kalamees T, Abadie MO, Steeman M, Kalagasidis AS. The effect of combining a relative-humidity-sensitive ventilation system with the moisture-buffering capacity of materials on indoor climate and energy efficiency of buildings. *Building and Environment* 2009; **44**: 515-524.

[9] Engelund ET, Thygesen LG, Svensson S, Hill CAS. A critical discussion of the physics of wood-water interactions. *Wood Science and Technology* 2013; **47**: 141-161.

[10] Time B. *Hygroscopic moisture, transport in wood*. Norwegian University of Science and Technology Trondheim, 1998.

[11] Leuk P, Schneeberger M, Hirn U, Bauer W. Heat of sorption: A comparison between isotherm models and calorimeter measurements of wood pulp. *Drying Technology* 2016; **34**: 563-573.

[12] Childs P, Greenwood J, Long C. Review of temperature measurement. *Review of Scientific Instruments* 2000; **71**: 2959-2978.

[13] Reszka P, Torero JL. In-depth temperature measurements in wood exposed to intense radiant energy. *Experimental Thermal and Fluid Science* 2008; **32**: 1405-1411.

[14] Tran, C. & White, R. Burning Rate of Solid Wood Measured in a Heat Release Rate Calorimeter 1992; **Fire and Materials 16**: 197-206.

[15] FLIR Systems. FLIR E60 Datasheet 2014; **26.03.2017**: http://www.infraredcamerawarehouse.com/content/FLIR%20Datasheets/FLIR%20E60%20Datasheet.pdf.

[16] Gade R, Moeslund TB. Thermal cameras and applications: a survey. *Machine Vision and Applications* 2014; **25**: 245-262.

[17] Fokaides PA, Jurelionis A, Gagyte L, Kalogirou SA. Mock target IR thermography for indoor air temperature measurement. *Applied Energy* 2016; **164**: 676-685.

[18] Usamentiaga R, Venegas P, Guerediaga J, Vega L, Molleda J, Bulnes FG. Infrared Thermography for Temperature Measurement and Non-Destructive Testing. *Sensors* 2014; **14**: 12305-12348.

[19] Vollmer M, Mollmann KP. *Infrared Thermal Imaging: Fundamentals, Research and Applications*. Wiley: Weinheim, Germany, 2011.

[20] Madding R. Emissivity measurement and temperature correction accuracy considerations. *Thermosense Xxi* 1999; **3700**: 393-401.

[21] The International Organization for Standardization (ISO). ISO 18434-1:2008. Condition monitoring and diagnostics of machines–Thermography–Part 1: General procedures 2011;.

[22] American Society of Testing and Materials (ASTM). ASTM E1933 - 99a. Standard Test Methods for Measuring and Compensating for Emissivity Using Infrared Imaging Radiometers 1999;.

[23] Lopez G, Basterra LA, Acuna L, Casado M. Determination of the Emissivity of Wood for Inspection by Infrared Thermography. *Journal of Nondestructive Evaluation* 2013; **32**: 172-176.

[24] American Society of Testing and Materials (ASTM). ASTM E1862. Measuring and compensating for reflected apparent temperature using infrared imaging radiometers 1998;.

[25] FLIR Systems. Infrared camera accuracy and uncertainty in plain language 2016; **2017**: http://www.flir.com/science/blog/details/?ID=74935.

[26] Chrzanowski K, Fischer J, Matyszkiel R. Testing and evaluation of thermal cameras for absolute temperature measurement. *Optical Engineering* 2000; **39**: 2535-2544.

[27] Chrzanowski K, Matyszkiel R, Fischer J, Barela J. Uncertainty of temperature measurement with thermal cameras. *Optical Engineering* 2001; **40**: 1106-1114.

[28] Minkina W, Dudzik S. Simulation analysis of uncertainty of infrared camera measurement and processing path. *Measurement* 2006; **39**: 758-763.

[29] Kylili A, Fokaides PA, Christou P, Kalogirou SA. Infrared thermography (IRT) applications for building diagnostics: A review. *Applied Energy* 2014; **134**: 531-549.

[30] Lahiri BB, Bagavathiappan S, Jayakumar T, Philip J. Medical applications of infrared thermography: A review. *Infrared Physics & Technology* 2012; **55**: 221-235.

[31] Purohit RC, Turner TA, Pascoe DD. Use of infrared imaging in veterinary medicine. *Biomedical Signals, Imaging, and Informatics*. CRC Press, 2014:1158-1165.

[32] Bogue R. Sensors for condition monitoring: a review of technologies and applications. *Sensor Review* 2013; **33**: 295-299.

[33] Ibarra-Castanedo C, Tarpani JR, Maldague XPV. Nondestructive testing with thermography. *European Journal of Physics* 2013; **34**: S91-S109.

[34] Hong T, Koo C, Kim J, Lee M, Jeong K. A review on sustainable construction management strategies for monitoring, diagnosing, and retrofitting the building's dynamic energy performance: Focused on the operation and maintenance phase. *Applied Energy* 2015; **155**: 671-707.

[35] Gonzalez-Aguilera D, Lagueela S, Rodriguez-Gonzalvez P, Hernandez-Lopez D. Image-based thermographic modeling for assessing energy efficiency of buildings facades. *Energy and Buildings* 2013; **65**: 29-36.

[36] Arora N, Martins D, Ruggerio D, Tousimis E, Swistel AJ, Osborne MP, Simmons RM. Effectiveness of a noninvasive digital infrared thermal imaging system in the detection of breast cancer. *American Journal of Surgery* 2008; **196**: 523-526.

[37] Chou Y, Yao L. Automatic diagnostic system of electrical equipment using infrared thermography 2009;: 155-160.

[38] La Rosa G, Risitano A. Thermographic methodology for rapid determination of the fatigue limit of materials and mechanical components. *International Journal of Fatigue* 2000; **22**: 65-73.

[39] FLIR Systems. User's manual - FLIR Exx series 2013; **2017**: http://www.flir-direct.com/pdfs/cache/www.flir-direct.com/flir_systems/thermal_imager/e60/manual/flir_systems_e60_thermal_imager_manual.pdf.

[40] Kollman FFP, Côté WA. *Principles of wood science and technology: solid wood*. Allen & Unwin, 1968.

[41] Dupleix A, Meneses DDS, Hughes M, Marchal R. Mid-infrared absorption properties of green wood. *Wood Science and Technology* 2013; **47**: 1231-1241.

[42] Kortelainen K, Vahtikari K, Noponen T, Hughes M. An investigation into the surface temperature changes in solid wood during sorption. Aalto University - School of Chemical Technology 2015;.

[43] Wood Science. Wood Science: Structure of wood: Basic knowledge: Macroscopic structure of wood 2014; **26.03.2017**: https://is.mendelu.cz/eknihovna/opory/index.pl?cast=19203.

Appendix 1 Temperature change during adsorption on transverse specimens

1.

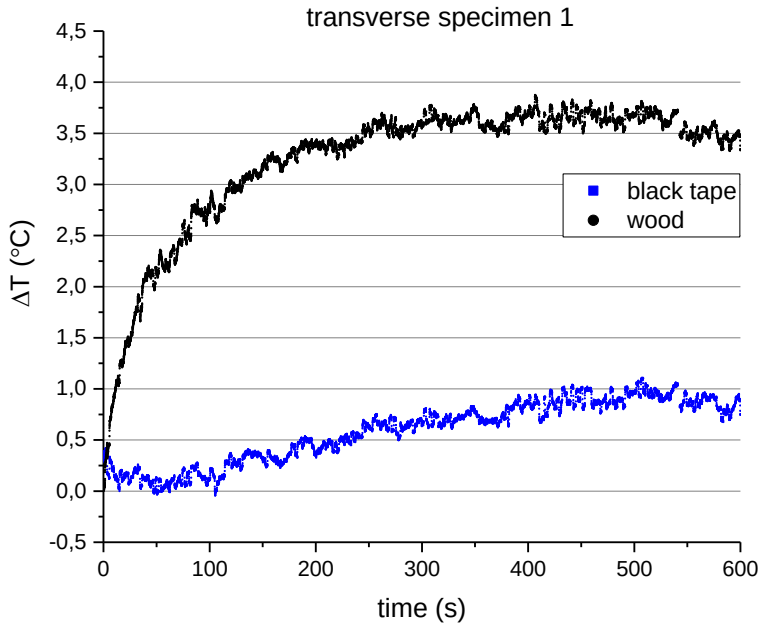

2.

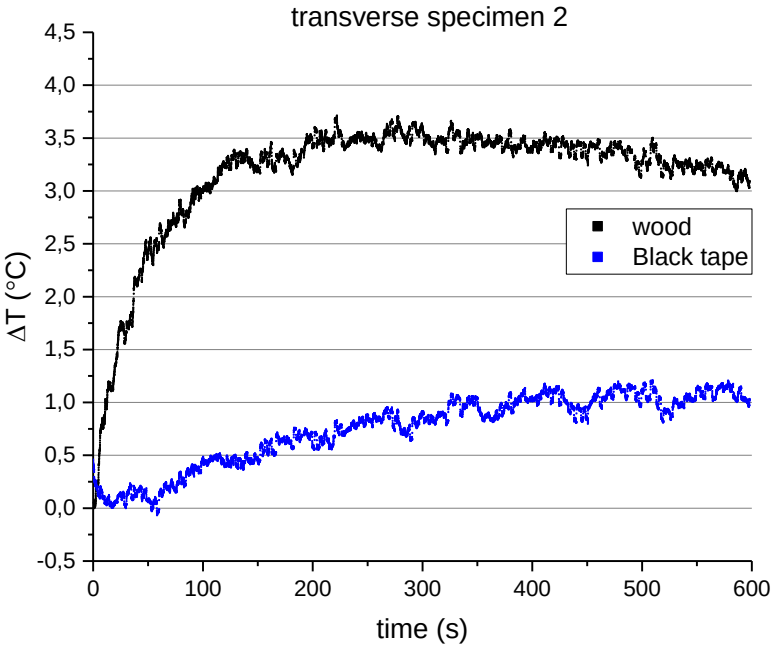

3.

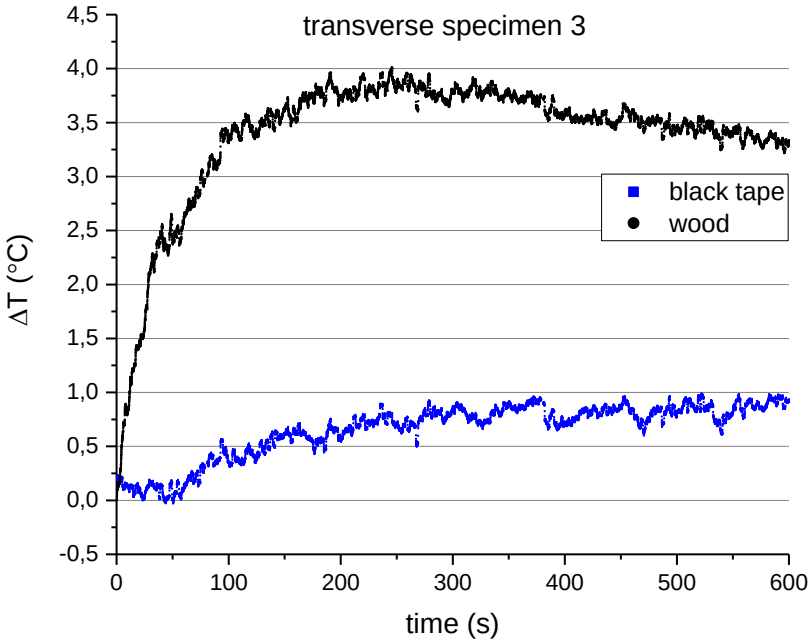
transverse specimen 3
ΔT (°C)
time (s)
black tape
wood
4,5
4,0
3,5
3,0
2,5
2,0
1,5
1,0
0,5
0,0
-0,5
0
100
200
300
400
500
600

4.

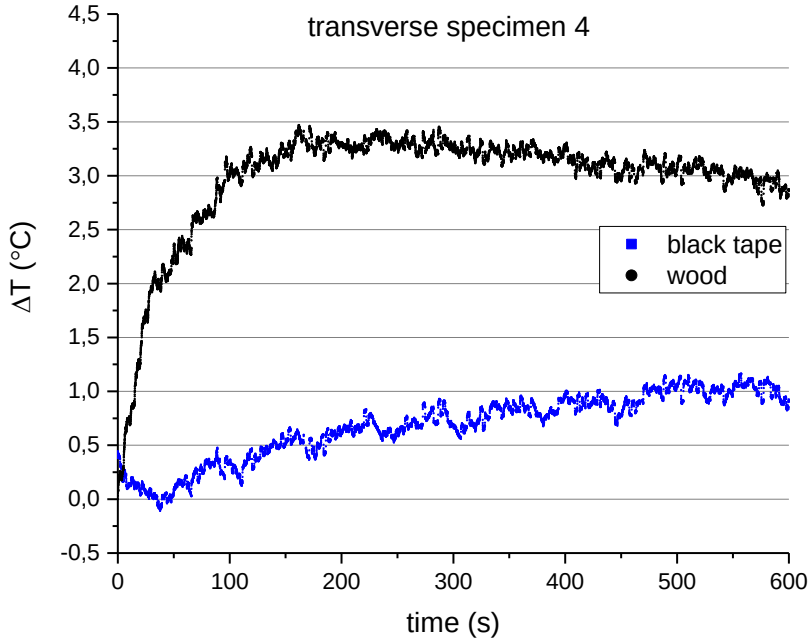
transverse specimen 4
ΔT (°C)
time (s)
black tape
wood
4,5
4,0
3,5
3,0
2,5
2,0
1,5
1,0
0,5
0,0
-0,5
0
100
200
300
400
500
600

5.

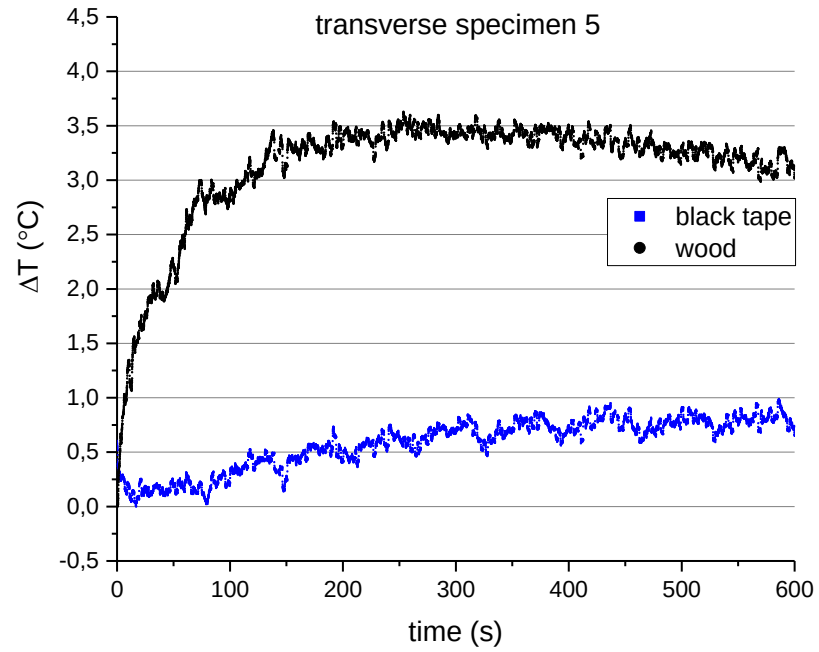
transverse specimen 5
ΔT (°C)
time (s)
black tape
wood
4,5
4,0
3,5
3,0
2,5
2,0
1,5
1,0
0,5
0,0
-0,5
0
100
200
300
400
500
600

6.

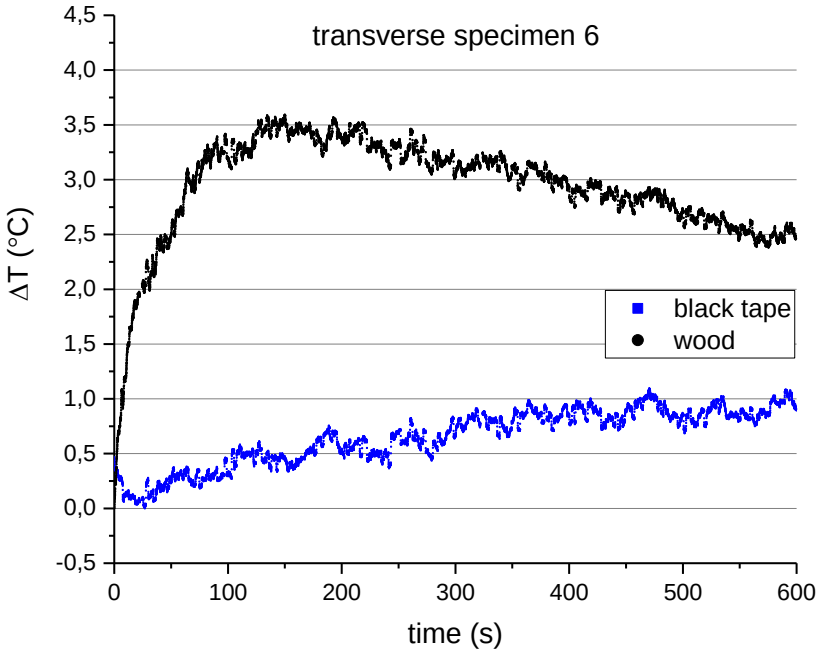
transverse specimen 6
ΔT (°C)
time (s)
black tape
wood
4,5
4,0
3,5
3,0
2,5
2,0
1,5
1,0
0,5
0,0
-0,5
0
100
200
300
400
500
600

7.

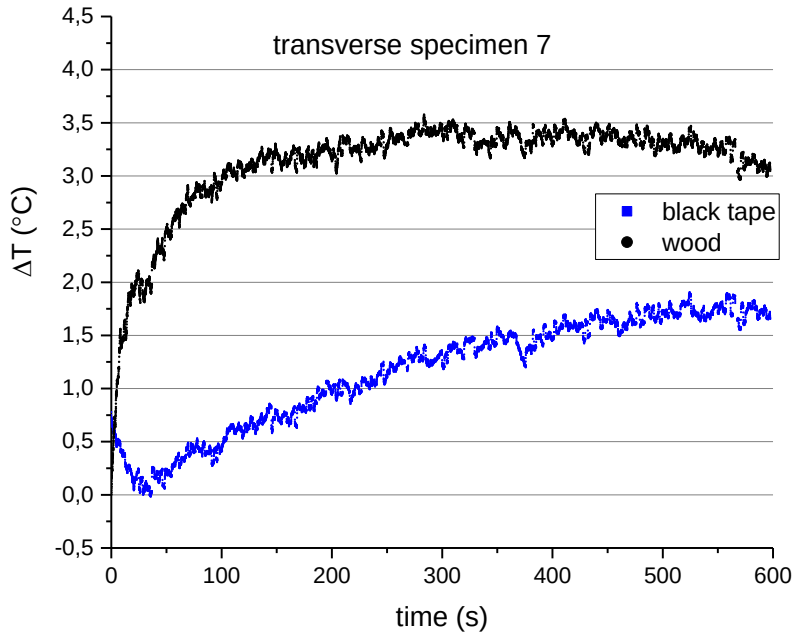
transverse specimen 7
ΔT (°C)
time (s)
black tape
wood
4,5
4,0
3,5
3,0
2,5
2,0
1,5
1,0
0,5
0,0
-0,5
0
100
200
300
400
500
600

8.

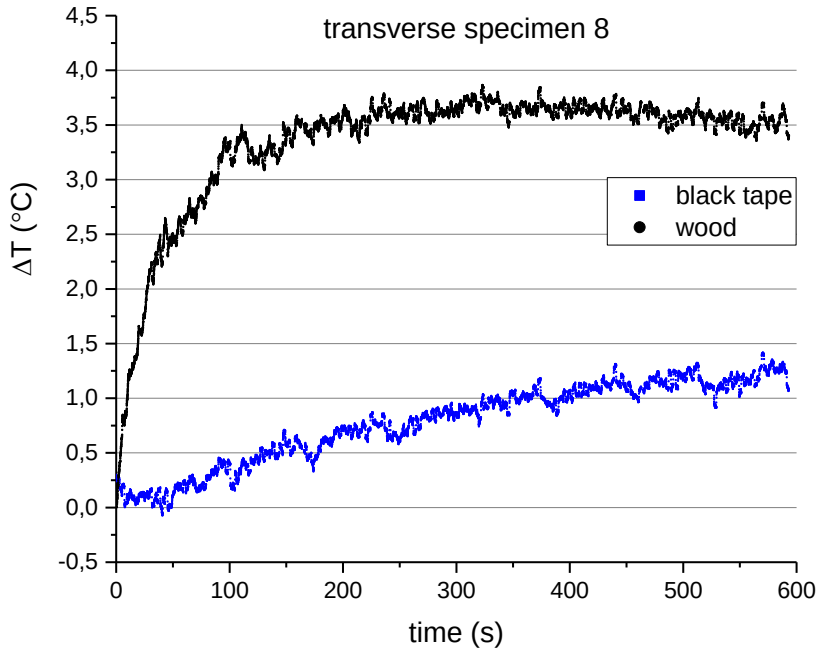
transverse specimen 8
ΔT (°C)
time (s)
black tape
wood
4,5
4,0
3,5
3,0
2,5
2,0
1,5
1,0
0,5
0,0
-0,5
0
100
200
300
400
500
600

9.

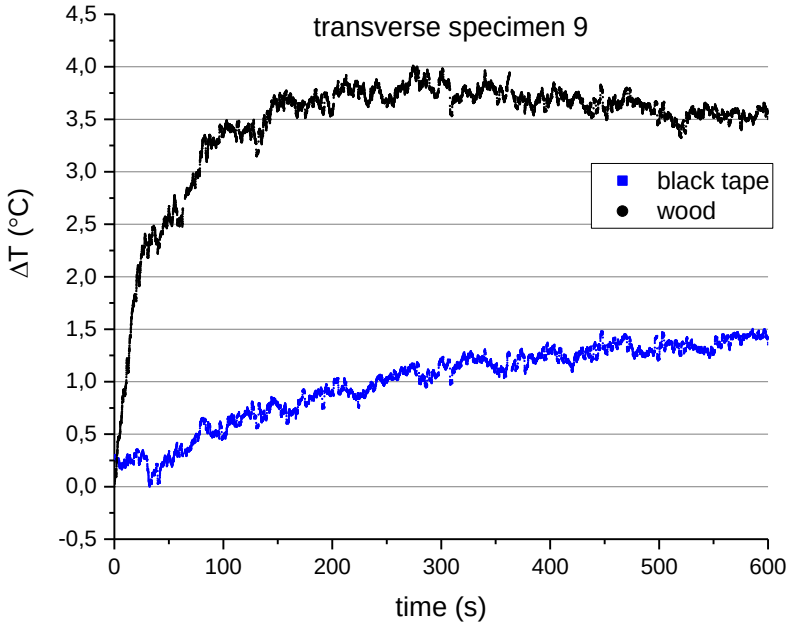
transverse specimen 9
ΔT (°C)
time (s)
black tape
wood
4,5
4,0
3,5
3,0
2,5
2,0
1,5
1,0
0,5
0,0
-0,5
0
100
200
300
400
500
600

10.

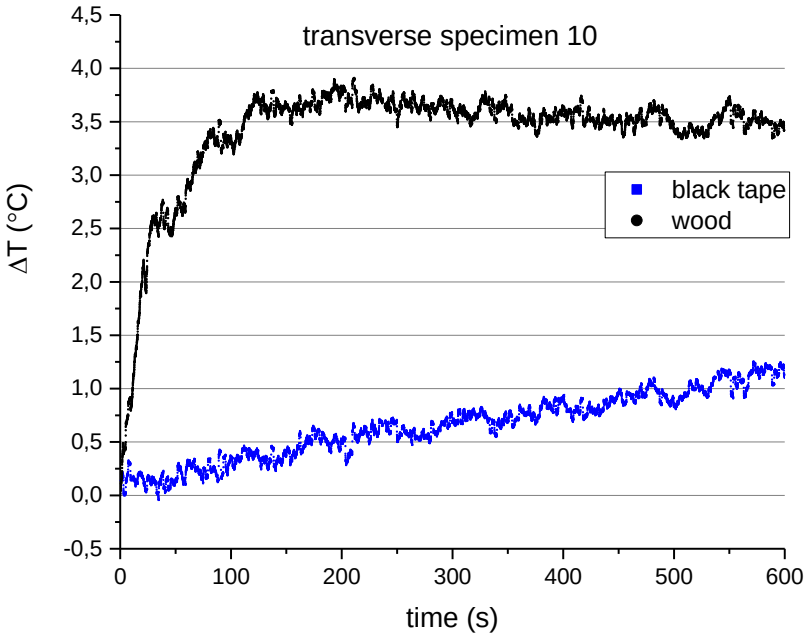
transverse specimen 10
ΔT (°C)
time (s)
black tape
wood
4,5
4,0
3,5
3,0
2,5
2,0
1,5
1,0
0,5
0,0
-0,5
0
100
200
300
400
500
600

Appendices 2 Temperature change during adsorption on tangential specimens

1.

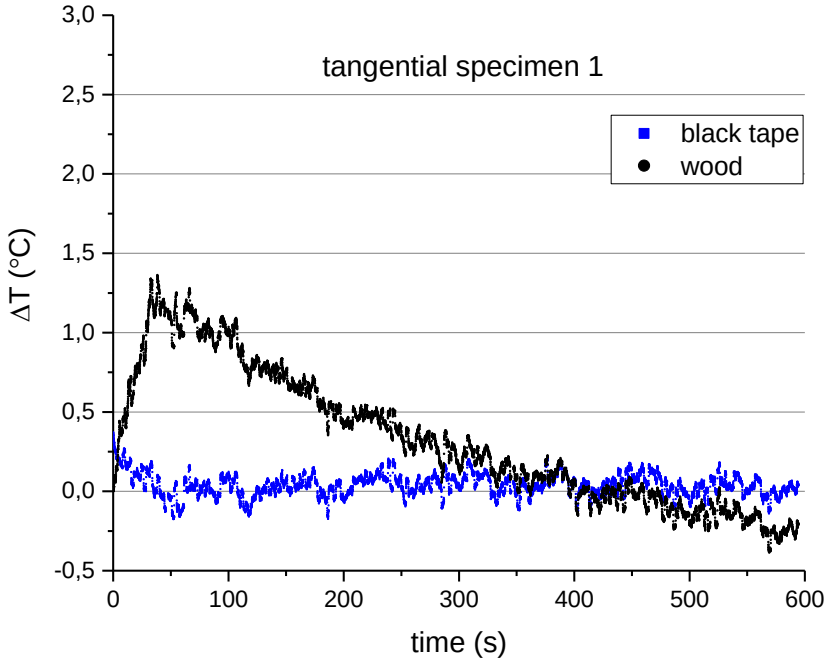

2.

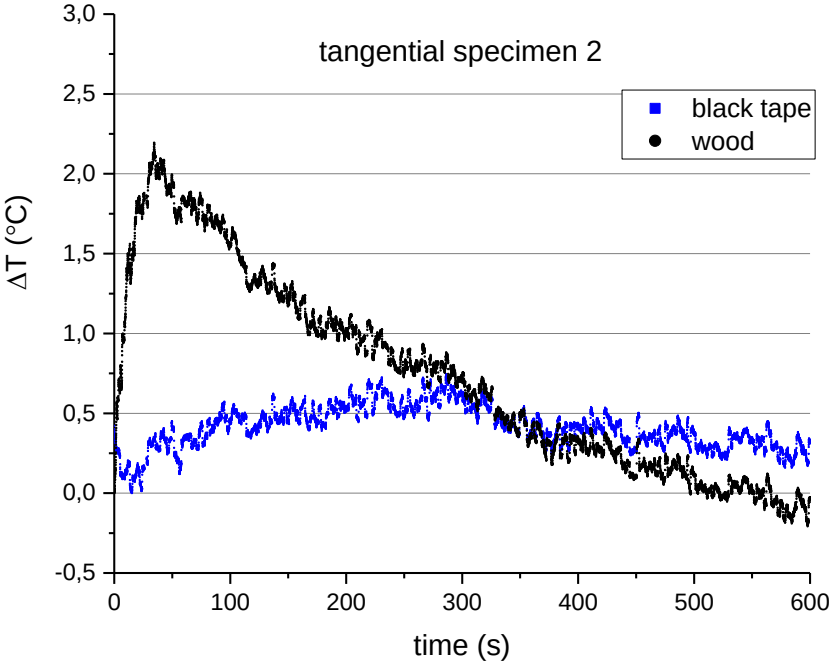

3.

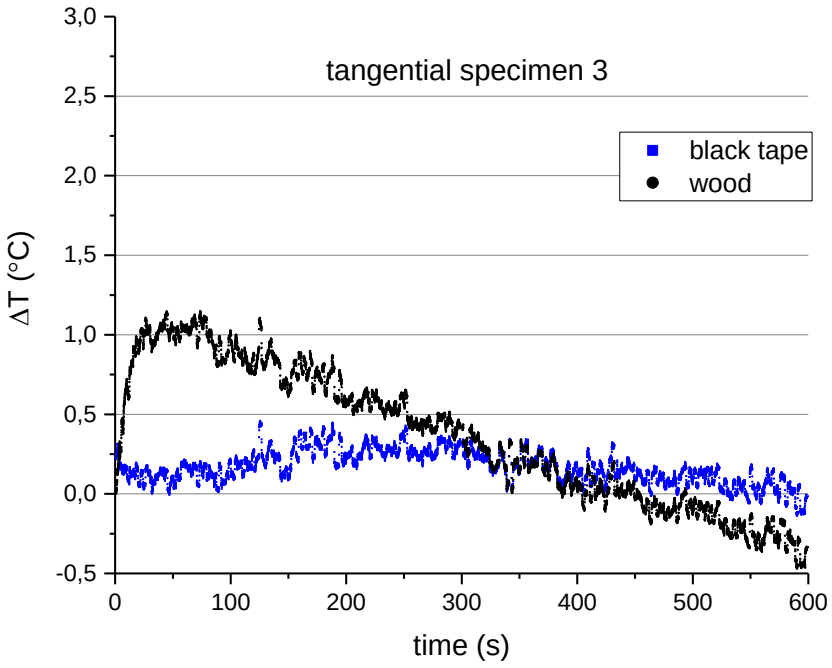
tangential specimen 3
black tape
wood
ΔT (°C)
time (s)
3,0
2,5
2,0
1,5
1,0
0,5
0,0
-0,5
0
100
200
300
400
500
600

4.

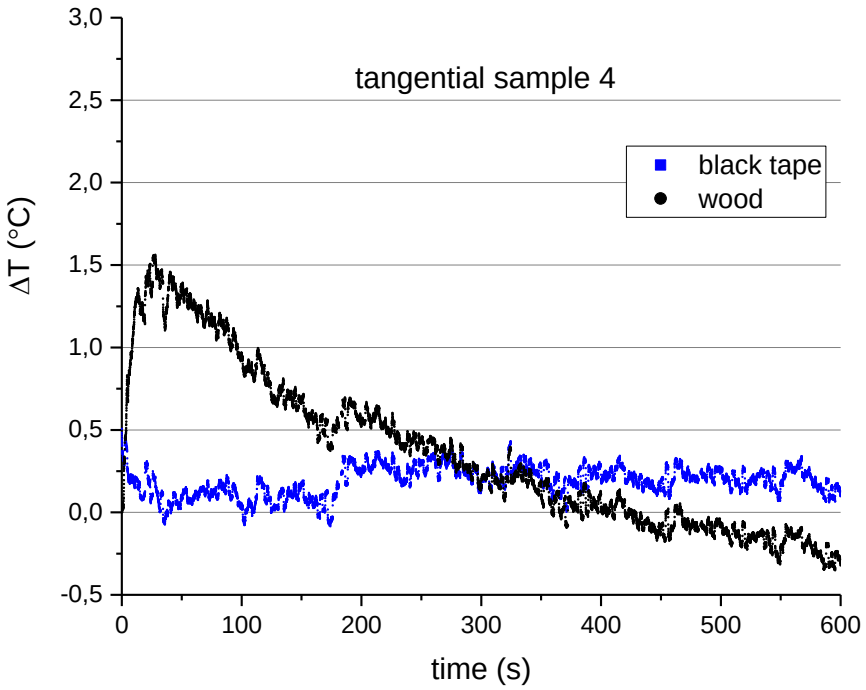
tangential sample 4
black tape
wood
ΔT (°C)
time (s)
3,0
2,5
2,0
1,5
1,0
0,5
0,0
-0,5
0
100
200
300
400
500
600

5.

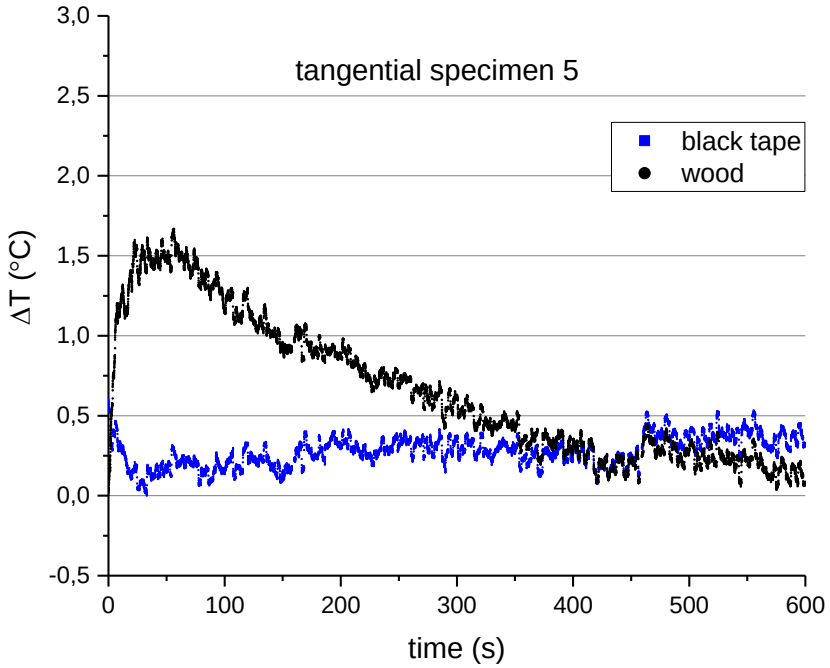
tangential specimen 5
black tape
wood
ΔT (°C)
time (s)
3,0
2,5
2,0
1,5
1,0
0,5
0,0
-0,5
0
100
200
300
400
500
600

6.

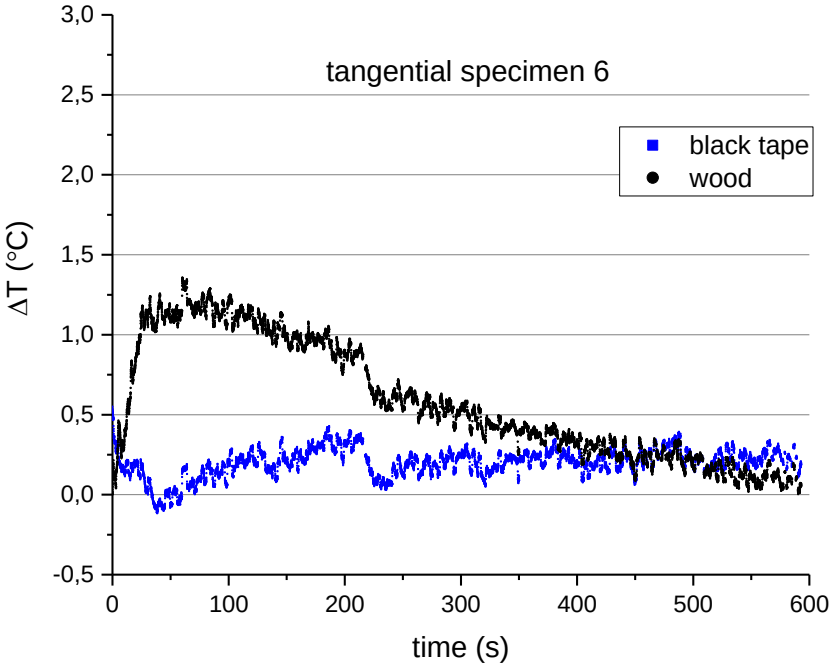
tangential specimen 6
black tape
wood
ΔT (°C)
time (s)
3,0
2,5
2,0
1,5
1,0
0,5
0,0
-0,5
0
100
200
300
400
500
600

7.

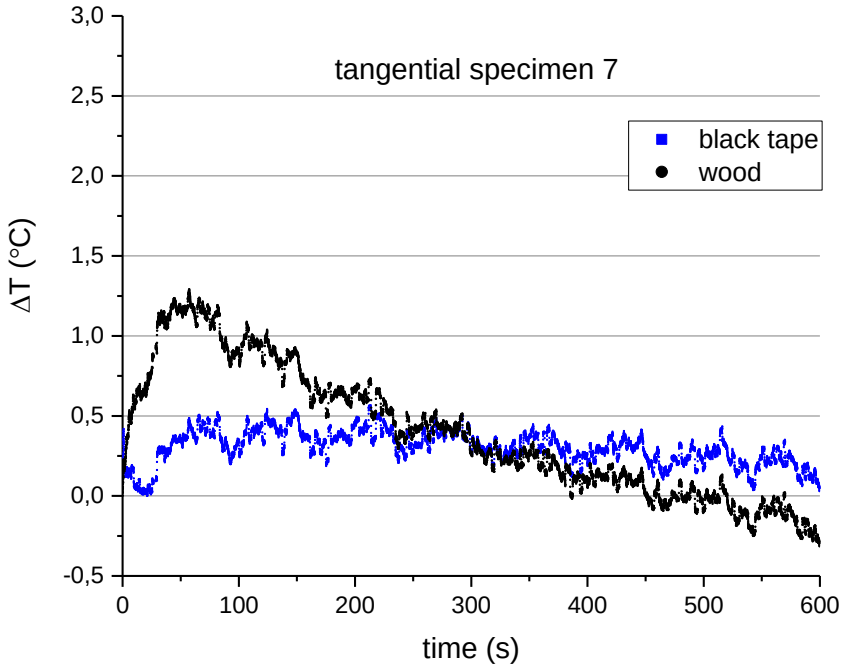
tangential specimen 7
black tape
wood
ΔT (°C)
time (s)
3,0
2,5
2,0
1,5
1,0
0,5
0,0
-0,5
0
100
200
300
400
500
600

8.

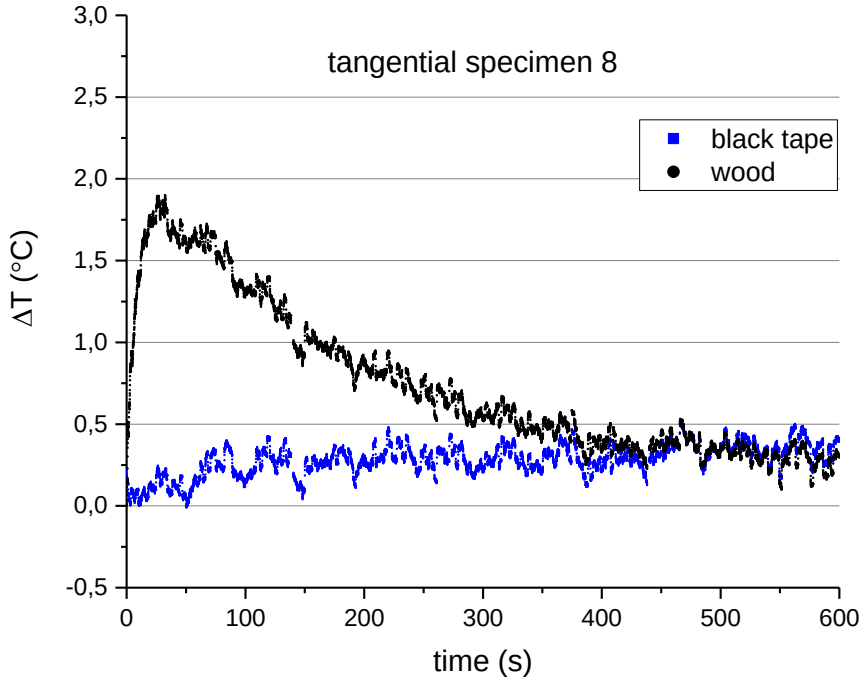
tangential specimen 8
black tape
wood
ΔT (°C)
time (s)
3,0
2,5
2,0
1,5
1,0
0,5
0,0
-0,5
0
100
200
300
400
500
600

9.

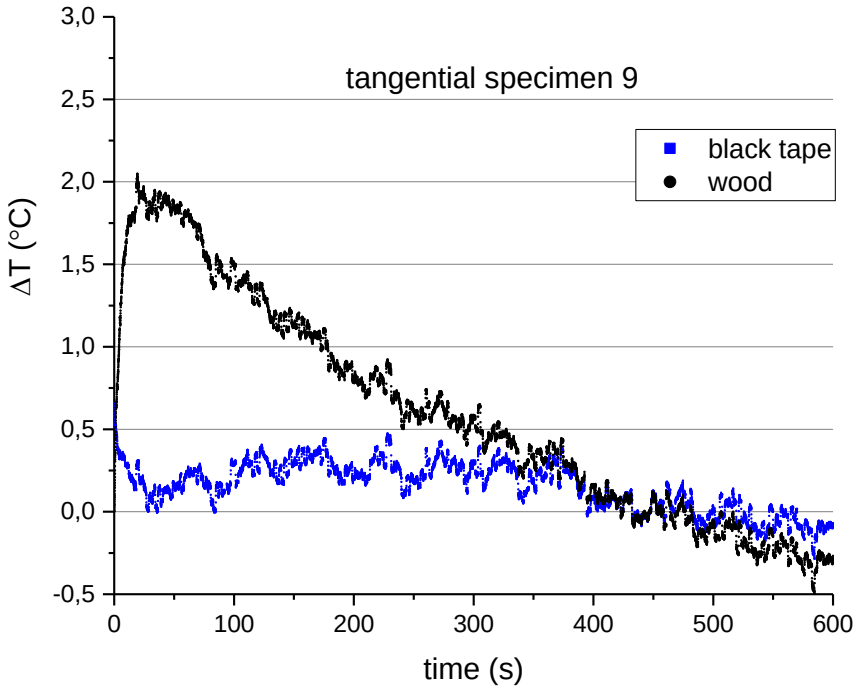
tangential specimen 9
black tape
wood
ΔT (°C)
time (s)
3,0
2,5
2,0
1,5
1,0
0,5
0,0
-0,5
0
100
200
300
400
500
600

10.

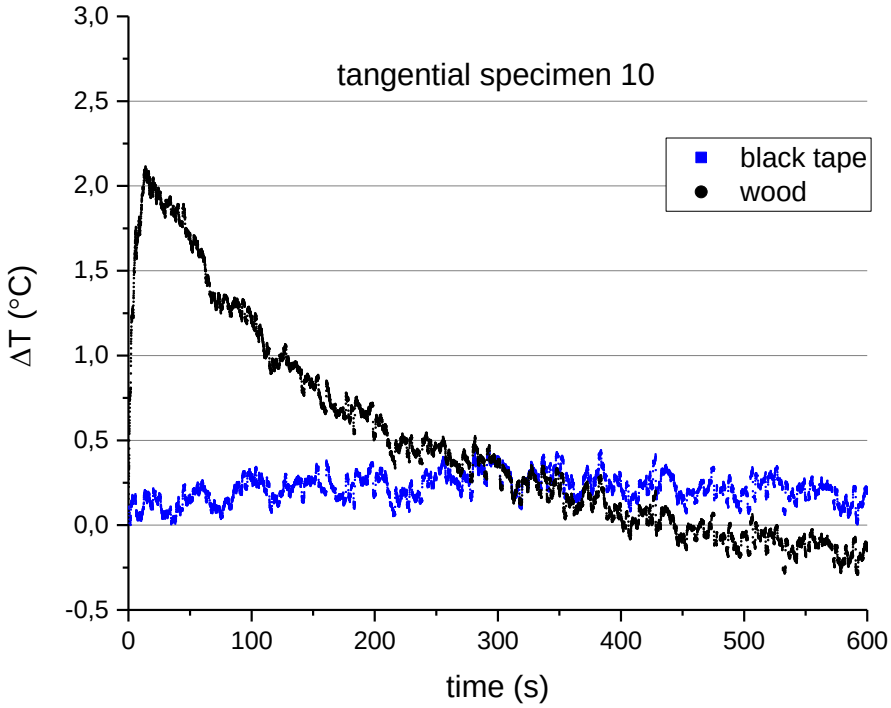
tangential specimen 10
black tape
wood
ΔT (°C)
time (s)
3,0
2,5
2,0
1,5
1,0
0,5
0,0
-0,5
0
100
200
300
400
500
600

Appendices 3 Temperature change during adsorption on radial specimens

1.

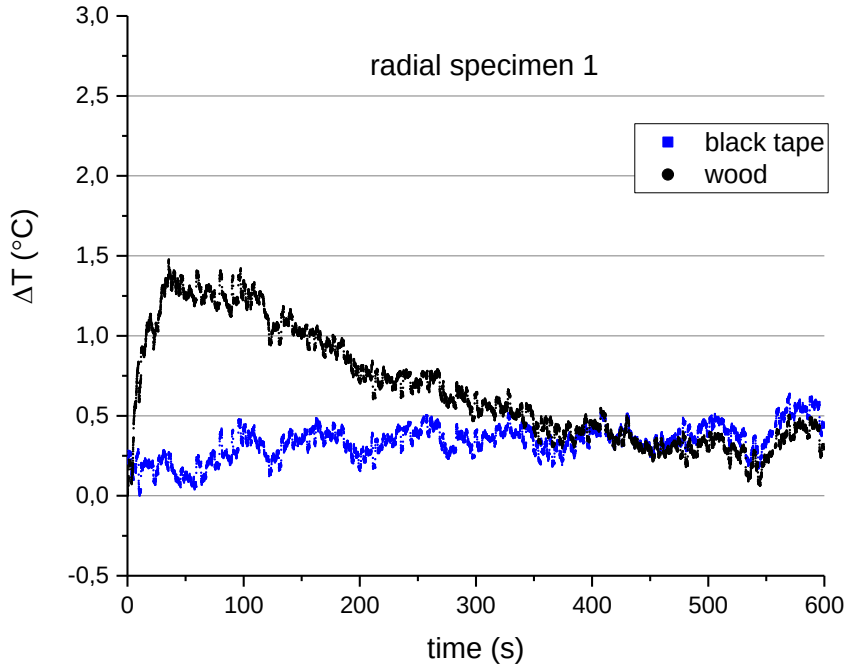

2.

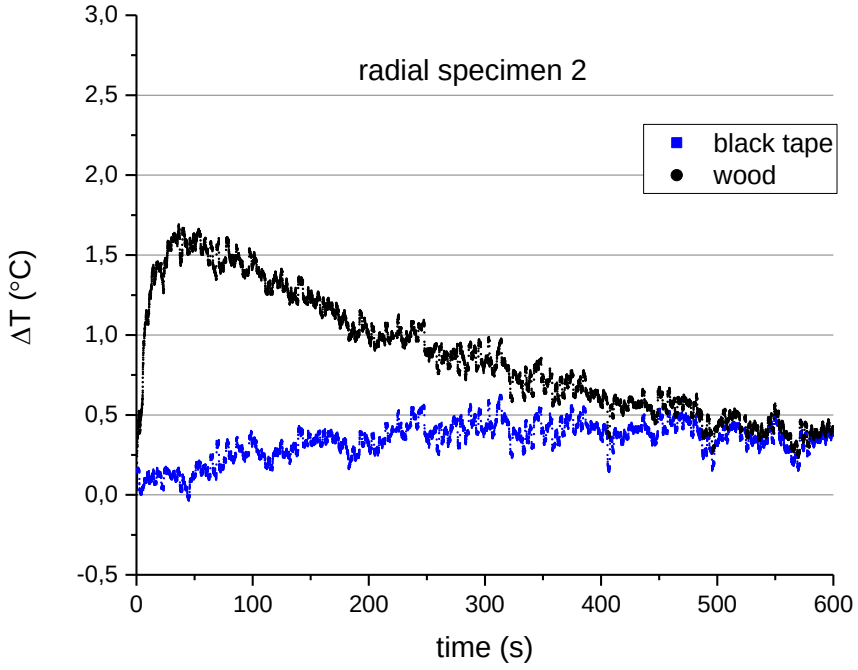

3.

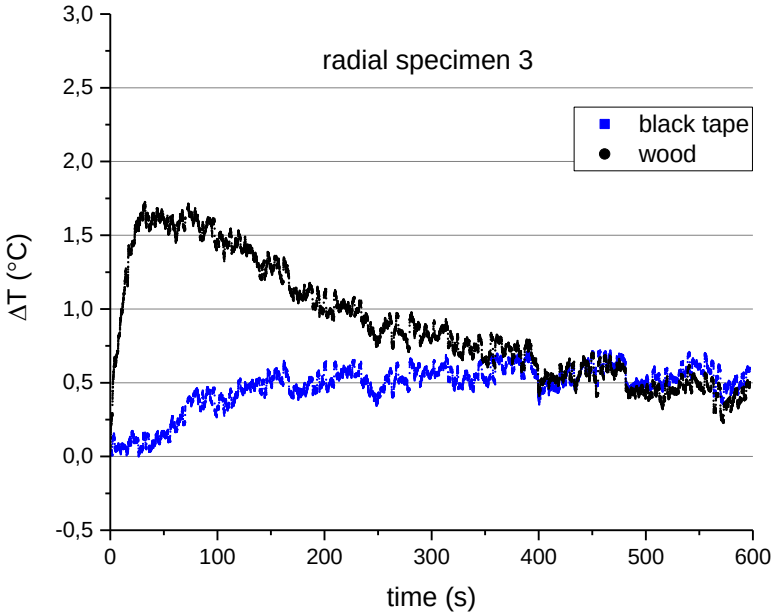
radial specimen 3
black tape
wood
ΔT (°C)
time (s)
3,0
2,5
2,0
1,5
1,0
0,5
0,0
-0,5
0
100
200
300
400
500
600

4.

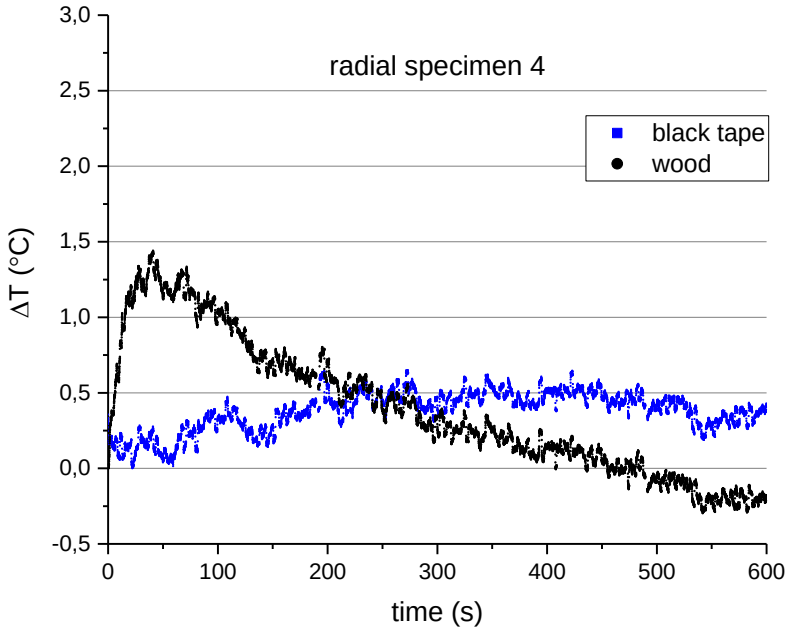
radial specimen 4
black tape
wood
ΔT (°C)
time (s)
3,0
2,5
2,0
1,5
1,0
0,5
0,0
-0,5
0
100
200
300
400
500
600

5.

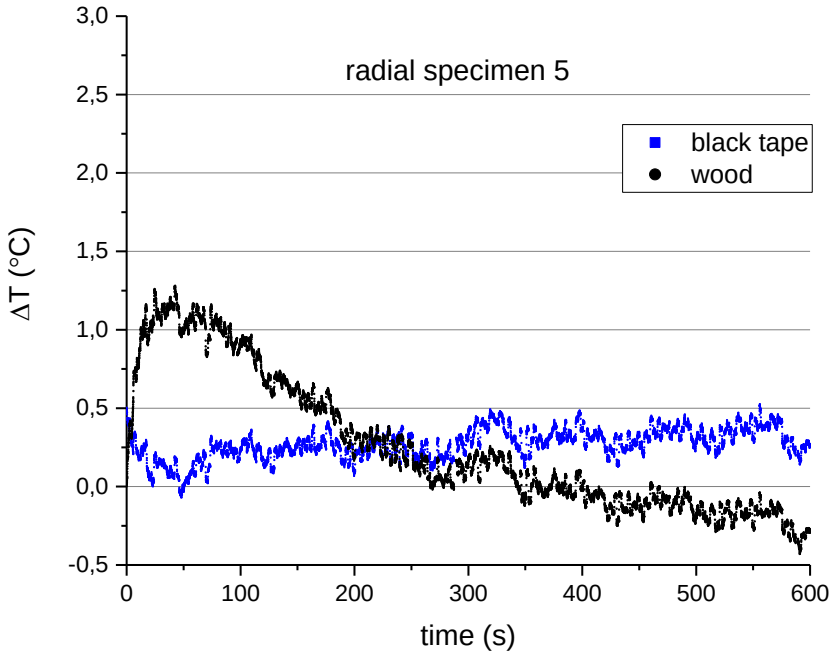
radial specimen 5
black tape
wood
ΔT (°C)
time (s)
3,0
2,5
2,0
1,5
1,0
0,5
0,0
-0,5
0
100
200
300
400
500
600

6.

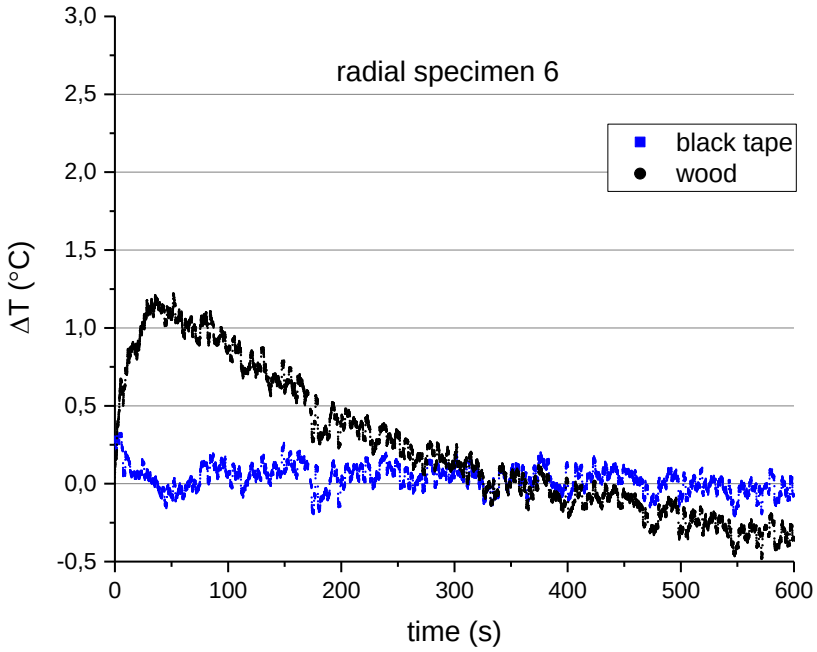
radial specimen 6
black tape
wood
ΔT (°C)
time (s)
3,0
2,5
2,0
1,5
1,0
0,5
0,0
-0,5
0
100
200
300
400
500
600

7.

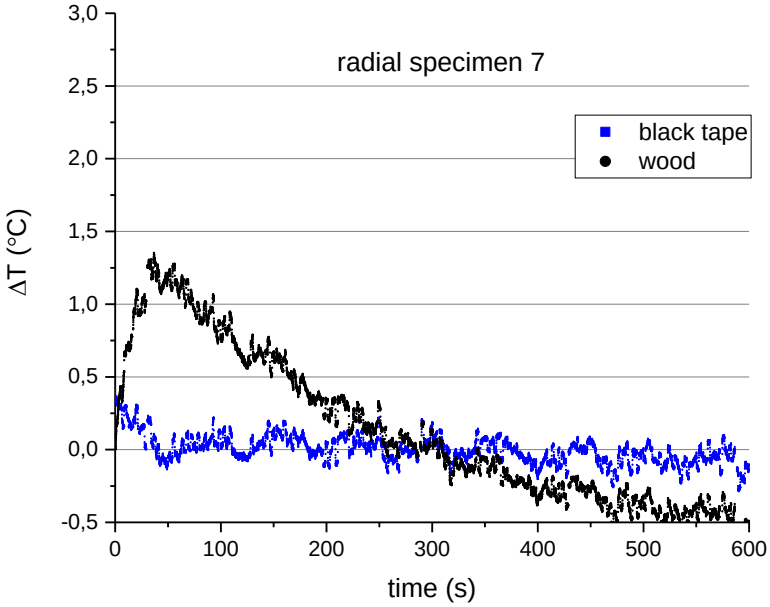
radial specimen 7
black tape
wood
ΔT (°C)
time (s)
3,0
2,5
2,0
1,5
1,0
0,5
0,0
-0,5
0
100
200
300
400
500
600

8.

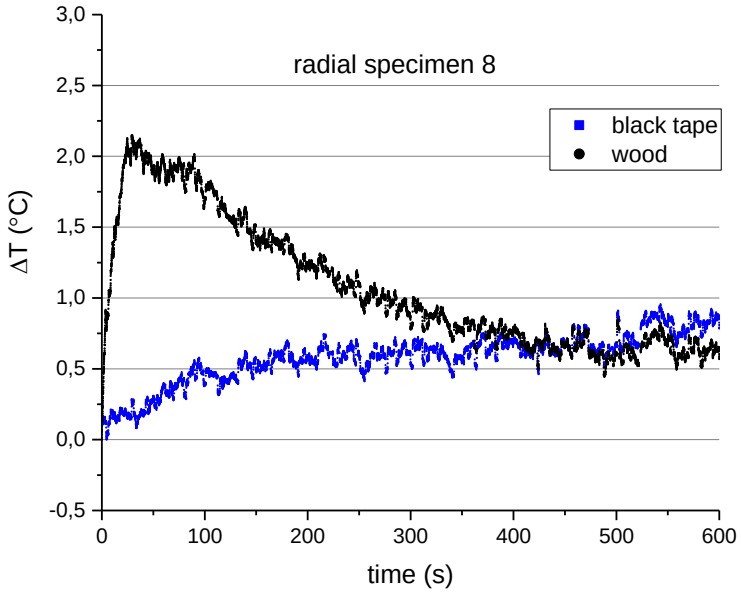
radial specimen 8
black tape
wood
ΔT (°C)
time (s)
3,0
2,5
2,0
1,5
1,0
0,5
0,0
-0,5
0
100
200
300
400
500
600

9.

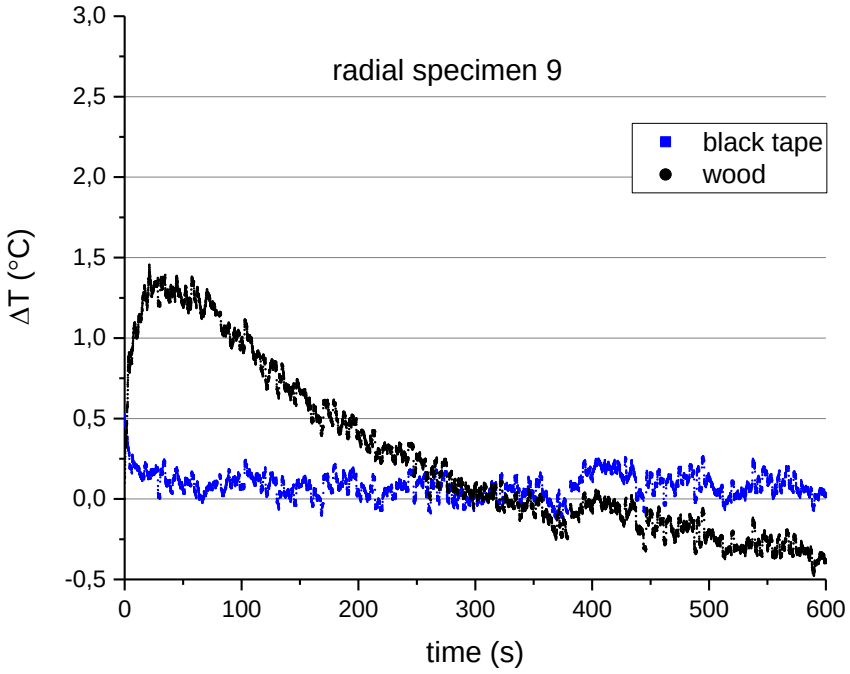
radial specimen 9
black tape
wood
ΔT (°C)
time (s)
3,0
2,5
2,0
1,5
1,0
0,5
0,0
-0,5
0
100
200
300
400
500
600

10.

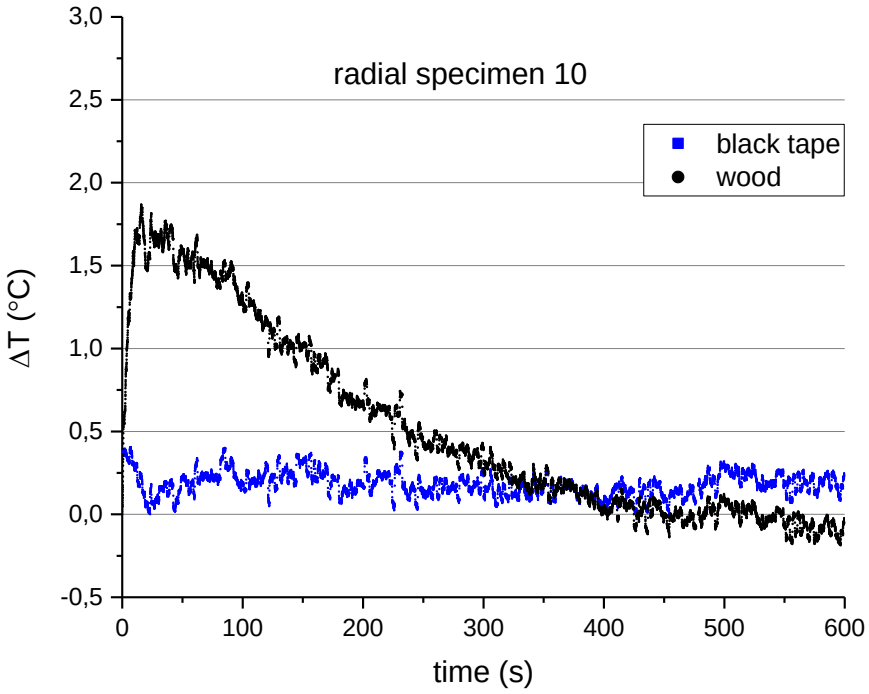
radial specimen 10
black tape
wood
ΔT (°C)
time (s)
3,0
2,5
2,0
1,5
1,0
0,5
0,0
-0,5
0
100
200
300
400
500
600